Geochimica et Cosmochimica Acta, Vol. 69, No. 10, pp. 2559–2579, 2005

0016-7037/05 $30.00 + .00

doi:10.1016/j.gca.2004.11.003

High-resolution geochemical record of Cretaceous-Tertiary boundary sections in Mexico: New constraints on the K/T and Chicxulub events

D. Stüben,[1,*] U. Kramar,[1] M. Harting,[1] W. Stinnesbeck,[2] and G. Keller[3]

[1]Institut für Mineralogie und Geochemie, Universität Karlsruhe, D-76128 Karlsruhe, Germany
[2]Geologisches Institut, Universität Karlsruhe, D-76128 Karlsruhe, Germany
[3]Department of Geosciences, Princeton University, Princeton, NJ 08544, USA

(*Received December* 22, 2003; *accepted in revised form November* 3, 2004)

Abstract—The investigation of eight Cretaceous–Tertiary (K/T) sections in Mexico, based on major and trace element, platinum group element (PGE), stable isotope, and multivariate statistical analysis, reveals a complex depositional history across the Chicxulub and K/T boundary events. At the biostratigraphically determined K/T boundary, a minor but significant Ir-dominated PGE anomaly (0.2–0.8 ng/g) is present in most sections. This Ir anomaly originated from an impact event and is always stratigraphically and geochemically decoupled from the underlying spherule-rich ejecta deposit related to the Chicxulub event. In all sections examined, one to three glass spherule ejecta layers and one or two chondrite-dominated PGE anomalies are separated by a bioturbated siliciclastic deposit and/or hemipelagic marl, which indicates the occurrence of at least two impact events separated by a considerable amount of time. In addition, bentonite layers and Pt and Pd-dominated PGE anomalies below and above the K/T boundary indicate volcanic activity. Above the K/T boundary, reduced bioproductivity is documented by a decrease in the biogenically bound fraction of nutrients and fluctuating ratios of immobile elements (e.g., Ti/Zr). Variations in detrital elements reflect changes in the depositional environment. Carbon and oxygen isotope and trace element distribution patterns indicate a gradually changing climate during the latest Maastrichtian, an abrupt change at the K/T boundary, and a slight recovery during the lowermost Paleocene.

1. INTRODUCTION

Environmental conditions before, during and after the Chicxulub impact event are still controversial despite analyses of numerous Cretaceous–Tertiary (K/T) boundary sections throughout Central America and the Caribbean by various research groups (Smit et al., 1992, 1996; Bohor and Betterton, 1993; Smit, 1999; Bohor, 1996; Stinnesbeck et al., 1993; Stinnesbeck and Keller, l996; Claeys et al., 2002; Keller et al., 2002a,c, 2003, 2004a,b). Aspects central to this controversy concern the exact stratigraphic position of the K/T boundary, the age and depositional nature of impact spherules, and the nature and emplacement of marls and siliciclastic sediments that characteristically separate the K/T boundary from the underlying impact spherules. Understanding these aspects is critical to resolving the current controversy regarding the age of the Chicxulub impact, as well as the role it may have played in the end-Cretaceous mass extinction and climate changes. High-resolution geochemistry of K/T sections in Central America can help resolve these issues.

Here we report the results of a high-resolution geochemical investigation of eight K/T sequences from northeastern, east-central, and southern Mexico to reconstruct the nature of the K/T events and their environmental consequences. These sections have been considered critical (Alvarez et al., 1992; Smit et al., 1992; Bohor and Betterton, 1993; Bohor, 1996) to understanding the causes of the global mass extinction at the K/T boundary and the role of the Chicxulub impact, but only limited geochemical data exist. For instance, a K/T boundary Ir-anomaly has only been published to date from a single section at El Mimbral (Smit et al., 1992; Stinnesbeck et al., 1993), whereas in another section an Ir anomaly is observed above the K/T boundary (Stinnesbeck et al., 2002). The scarcity of K/T iridium data are largely due to the fact that in most outcrops the K/T and Tertiary sediments are eroded. Most studies have therefore concentrated on the siliciclastic and underlying spherule deposits (Schulte et al., 2003). A detailed mineralogical study of these deposits was published by Adatte et al. (1996).

This study reports on the platinum group element (PGE), major and trace element concentrations, and stable isotope ratios (oxygen and carbon) across sections spanning the K/T boundary, and places these into the context of current litho- and biostratigraphic knowledge. Our analysis provides new information regarding the age of the Chicxulub impact and its relationship to the K/T boundary, the stratigraphic position, and origin of Ir and other PGE anomalies, and climate change.

2. PREVIOUS WORK: GEOLOGY OF NE MEXICO K/T SECTIONS

During Maastrichtian and early Paleogene times, northeastern and central eastern Mexico received a steady influx of terrigenous clastic sediments from the rising Sierra Madre Oriental (Laramide phase of alpine orogeny) to the east, and from an extensive deltaic complex to the northwest (Sohl et al., 1991; Galloway and Williams, 1991) (Fig. 1, inset). Siliciclastic deltaic and pro-deltaic deposits of the Difunta Group characterize the region north and west of Saltillo, whereas distal pro-deltaic facies are located east and southeast of Monterrey. In this latter region, a moderately deep water shelf-slope region developed during the Maastrichtian and early Paleogene and

* Author to whom correspondence should be addressed (doris.stueben@img.uni-karlsruhe.de).

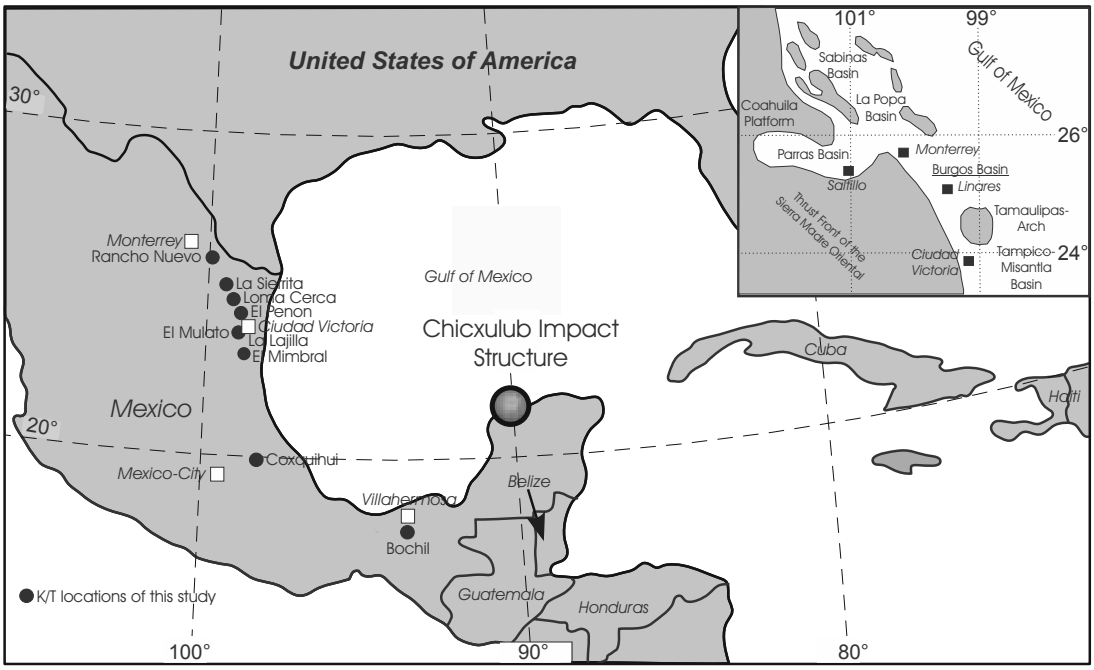

Fig. 1. Sketch map of the geographical positions of the investigated K/T sections Los Dos Plebes, Loma Cerca, El Peñon, El Mulato, La Lajilla, Mimbral, Coxquihui, and Bochil. Inset: Paleogeography of NE Mexico, for comparison.

more than 1000 m of rhythmically bedded marls and shales were deposited. These open marine sediments reached water depths of ~100 m near Los Ramones 40 km northeast of Monterrey (Stinnesbeck and Keller, 1996; Keller et al., 1997), more than 400 m in the Los Dos Plebes region 40 km east of Montemorelos (Keller et al., 1997; Stinnesbeck et al., 2001; Alegret et al., 2002) and ~200–350 m in the Mimbral area east of Ciudad Victoria (Keller et al., 1994).

2.1. Placement of K/T Boundary

Across this region, the K/T boundary is placed either below or above a massive siliciclastic deposit with a unit of spherule-rich sediments at the base. Placement of the K/T boundary below is based on the interpretation of the siliciclastic deposit as an impact ejecta and the siliciclastic deposit as a mega-tsunami deposit (Smit et al., 1992, 1996, Smit, 1999). In this scenario the spherule layer is thought to mark the K/T boundary. This single-event catastrophic interpretation, however, is not supported by the presence of multiple horizons of bioturbation within the siliciclastic deposits, as well as a burrowed limestone layer within the spherule layer, which indicate deposition occurred over an extended period of time during which benthic faunas repeatedly colonized the ocean floor (Keller et al., 1997; Ekdale and Stinnesbeck, 1998). In the alternative interpretation, the siliciclastic member is regarded as a long-term deposit, caused by a series of gravity flows or turbidity currents during the latest Maastrichtian sea level lowstand and also influenced by tectonic uplift in the Sierra Madre Oriental (Stinnesbeck et al., 1993; Stinnesbeck and Keller, 1996; Adatte et al., 1996). The K/T boundary is placed above the siliciclastic deposit and at the base of the Velasco Formation shales and marked by a small Ir anomaly and early Danian planktic foraminiferal assemblages indicative of zone P0 or P1a (*Parvularugoglobigerina eugubina,* Smit et al., 1992, 1996; Stinnesbeck et al., 1993, 2002; Stinnesbeck and Keller, 1996; Keller et al., 1994, 1997, 2002a, 2003; Smit, 1999; Soria et al., 2001). In this scenario, the spherule layers below the siliciclastic deposit represent an earlier impact event (Keller et al., 2002a, 2003).

2.2. The Siliclastic Deposit

The siliciclastic deposit varies in thickness from 0 cm to 11 m and consists of a spherule-rich unit 1 at the base, which frequently contains a 15–20-cm-thick limestone layer (Keller et al., 1997, 2003). Above unit 1 are thick sandstones (unit 2), and an alternating sandstone–siltstone complex (unit 3) forms the top. Animal burrows have been documented in the limestone layer of unit 1 and within units 2 and 3, which indicate deposition occurred over a long time period, rather than via impact-generated tsunami as commonly suggested (Smit et al., 1994, 1996; Smit, 1999). The spherule unit 1 overlies an undulating erosional surface of the Mendez marl Formation, which contains planktic foraminiferal assemblages of zone CF1 (*Plummerita hantkeninoides*).

2.3. Multiple Spherule Layers

Recent investigations of the late Maastrichtian sediment sequence below the disputed siliciclastic deposits with the unit 1 glass spherules at the base have revealed up to three additional glass spherule layers often separated by up to 6 m of Mendez Formation marls (Stinnesbeck et al., 2001; Keller et al., 2002a, 2003). In rare outcrops (e.g., Mesa Juan Perez), one or more glass spherule layers are syndepositionally deformed and

folded (Soria et al., 2001; Keller et al., 2002a,c; Schulte et al., 2003), but there is no evidence for regional large-scale slump deposits, earthquake-induced margin collapse, or any other significant tectonic activity. Recent investigations on spherule layers (e.g., El Peñon) revealed major differences in the physical (e.g., interstitial matrix) and chemical composition of unit 1 impact spherules and those from the underlying spherule layers within the Mendez marl (Keller et al., 2003; Harting, 2004). Harting (2004) documented a dramatic change from a detritus-free spherule layer within the Mendez marl to a detritus-rich unit 1 spherule layer with abundant shallow water microfossils (see also Keller et al., l994, 2003; Alegret et al., 2002) that clearly marks unit 1 as reworked and the stratigraphically oldest spherule layer near the base of zone CF1 as the original ejecta fallout. This study could not find any geochemical evidence in support of reworking due to slumping of unit 1, as proposed by Schulte (2003).

At Loma Cerca, as well as at El Peñon, the 4 to 5 m of marls between the reworked glass spherule layer of unit 1 and the stratigraphically oldest ejecta layer contain abundant and diverse planktic foraminifera, including *Plummerita hantkeninoides*, the index species of the latest Maastrichtian zone CF1 that spans the last 300 kyr of the Maastrichtian (Keller et al., 2002a, 2003). The first appearance of the index species is observed ~20 cm below the oldest spherule layer. This indicates that the glass spherules originated at ~65.3 Ma. Subsequent glass spherule layers appear to have been reworked from shallow water deposits and transported into deeper waters, as suggested by the abundance of shallow water detritus and foraminifera. Based on these data, Keller et al. (2002a, 2003) suggested that the Chicxulub impact occurred ~300,000 yr before the K/T boundary and that a second large impact coincided with the K/T mass extinction. Recent paleontological, magneto- and biostratigraphic, geochemical, and mineralogical investigations of the Yaxcopoil-1 core from the Chicxulub crater confirmed these observations, revealing that the Chicxulub impact occurred ~300,000 yr before the K/T mass extinction (Keller et al., 2004a,b). In contrast, Smit et al. (2004) and Arz et al. (2004) still maintain that Chicxulub is the K/T boundary impact and all sediments in between the impact ejecta and the K/T boundary are deposited due to tsunami waves or backwash.

3. MATERIALS AND METHODS

3.1. Locations of Sections Studied

The eight K/T boundary sections examined are located in eastern Mexico from the north to Chiapas in the south and parallel the present Gulf of Mexico coastline (Fig. 1). The sections span a 1500 km N-S transect from Los Dos Plebes (~70 km southeast of Monterrey, Nuevo Leon) to Bochil (Chiapas, southern Mexico). ~10 km SSE of Los Dos Plebes is the Loma Cerca section, one of the most expanded sequences. Both sections have bee extensively studied based on mineralogy and stratigraphy (Lindenmaier et al., 1999; Stinnesbeck et al., 2001; Keller et al., 2002a, 2003; Schulte et al., 2003). The classic El Peñon section is located ~35 km south of Loma Cerca and 100 km southeast of Monterrey/Nuevo Leon and has been extensively studied by Stinnesbeck et al. (1993, 1996), Keller et al. (1994, 1997, 2003), Adatte et al. (1996), Smit et al. (1996), and Smit (1999). Several outcrops are present in this area over a distance of ~500 m. The El Mulato outcrop is located ~150 km southeast of Monterrey/Nuevo Leon and 125 km north of Ciudad Victoria/Taumalipas (Fig. 1) and has been documented by Keller et al. (1994, 1997), Stinnesbeck and Keller (1996), Adatte et al. (1996), López-Oliva and Keller (1996), Smit et al. (1996), and Alegret et al. (2002). The La Lajilla section is located 40 km east of Ciudad Victoria, State of Tamaulipas, and along a river bed 200 m north of the village La Lajilla (Fig. 1). Previous studies were published by Stinnesbeck et al. (1993), Stinnesbeck and Keller (1996), Keller et al. (1994, 1997), Smit et al. (1996), and Adatte et al. (1996). The classic El Mimbral section is located 80 km southeast of Ciudad Victoria on the south bank of the Mimbral creek and has been studied by a number of investigators (Smit et al., 1992, 1996; Stinnesbeck et al., 1993, 1996; Keller et al., 1993, 1994, 1997, 2002a; Bohor, 1996; Adatte et al., 1996). To the south, in the central-east Mexico State of Veracruz, the Coxquihui section is located near the village of the same name 40 km west of Nautla. The section has been previously studied by Smit et al. (1996), Arz et al. (2001), and Stinnesbeck et al. (2002). In southern Mexico, the Bochil section is located 110 km south of Villahermosa (Fig. 1) in the state of Chiapas and has previously been studied by Montanari et al. (1994), Smit et al. (1996), Smit (1999), Grajales-Nishimura et al. (2000), and Keller et al. (2003).

At each section, samples of 100 to 200 g were taken for analysis at an average of 10-cm intervals and at 1- to 5-cm intervals across the K/T transition.

3.2. Biostratigraphy

Biostratigraphic age control is based on planktic foraminifera with methods detailed in Keller et al. (l995). The late Cretaceous sediments of all sections analyzed are within the *Plummerita hantkeninoides* zone CF1, which spans the last 300 kyr of the Maastrichtian. Early Tertiary sediments include the early Danian zones Pla to Plc, with zone P0 highly condensed (red layer) or missing. In most sections, zone Pla can be subdivided into subzones Pla(1) and Pla(2), based on the first appearances of *Parasubbotina pseudobulloides* or *Subbotina triloculinoides* (Keller et al., 2002a).

Criteria defining the K/T boundary have been established based on the official Global Stratotype Section and Point at El Kef, Tunisia (Cowie et al., 1989; Remane et al., 1999; Keller et al., 2002b). This section and the nearby co-stratotype at Elles represent the most complete and expanded sections known to date, and all other sections need to be compared to these standard sections in terms of completeness of the faunal and sedimentary record. At El Kef, the International Commission on Stratigraphy placed the boundary at the base of a 2-mm-thick red layer with maximum Ir concentrations and Ni-rich spinels, and a negative excursion in $\delta^{13}C$ values. The extinction of Maastrichtian tropical and subtropical planktic foraminifera occurs in the sediments immediately underlying the red clay, whereas *Globoconusa conusa* (= *P. extensa*) appears in the clay immediately overlying the red layer, and further Danian species (e.g., *Eoglobigerina fringa*, *E. edita*, *Woodringia hornerstownensis*) within a few centimeters upsection. The International Commission on Stratigraphy defined the K/T boundary on the basis of unique biomarkers, the mass extinction of Cretaceous species and first appearance of Danian species. All other criteria, including lithological changes, geochemical signals, Ir content, and Ni-rich spinels are additional markers to identify the boundary, but by themselves do not define it.

3.3. Bulk Chemical Analyses

Major and trace elements were determined by energy-dispersive and wavelength-dispersive X-ray fluorescence analysis at the Institut für Mineralogie und Geochemie, Universität Karlsruhe. By energy-dispersive X-ray fluorescence, 13 trace elements (Cu, Zn, Ga, As, Rb, Sr, Y, Zr, Nb, Cd, Sb, Ba, and Pb) were analyzed. For these determinations, an aliquot of ~5 g was used as bulk powder in polystyrol containers with a 6-μm Mylar window for measurement. The samples were measured 3 times with a SPECTRACE 5000 X-ray analyzer using Al, Pd, and Cu primary filters to optimize the excitation of elements emitting low, intermediate, and high X-ray energies, respectively. Details of the procedure are given in Kramar (1997). Detection limits obtained by energy-dispersive X-ray fluorescence in bulk rock powder are 5 μg/g for Cu, Zn, Zr, Ba, and Pb; 3 μg/g for Ga, As; 2 μg/g for Rb, Sr, Y, Nb; 1 and 0.5 μg/g for Sb and Cd, respectively. To validate the data, reference samples SGR-1, SOIL-5A, AGV-1, and GXR-2 were measured along with the samples. For drift control,

GXR-2 was included in each batch of 10 samples. For values greater than fivefold detection limit, the data generally agree within 10% with the reference values (Govindaraju, 1995).

Major and minor elements (Na, Al, Mg, Si, P, K, Ca, Ti, Mn, Fe) and some of the trace elements (V, Cr, and Ni) were determined by wavelength-dispersive X-ray fluorescence. Fused glass discs were prepared from a mixture of 1 g bulk powder and 4 g SPECTROMELT. The fused discs were analyzed with an SRS 303 AS wavelength-dispersive X-ray spectrometer with Rh tube excitation. Major and minor element data were evaluated by the fundamental parameter calibration procedure (Jenkins et al., 1981; Lachance and Claisse, 1995), whereas trace element abundances were determined using a combined Compton and intensity matrix correction procedure. To correct for matrix effects, the peak areas from trace elements with X-ray energies above the absorption edge of the heaviest major element (Fe) were normalized by the area of the Compton scattering. Trace elements below the absorption edge of Fe were also normalized to the Compton scattering, but matrix effects of Fe, Ti, and Ca were additionally corrected using the peak intensities of these elements (Intensity correction method, Lachance and Claisse, 1995). For all matrix correction procedures, calibration lines based on >20 reference rocks were prepared. Major and minor elements are reported as wt.% of their oxides.

Platinum group elements (PGE) were analyzed by high-resolution inductively coupled mass spectrometry at the Institut für Mineralogie und Geochemie, University of Karlsruhe after preconcentration and matrix reduction by Ni-fire assay (Kramar et al., 2001; Stüben et al., 2002). Before the fire assay procedure, samples were spiked with 500 μL of a solution containing 16 ng of Ir, 10 ng Ru, 33 ng Pd, and 33 ng Pt strongly enriched in the isotopes Ir^{191}, Ru^{99}, Pd^{105}, and Pt^{198}, respectively. The analysis was carried out by isotope dilution analysis (Taylor, 2000) and measured by high-resolution inductively coupled mass spectrometry (AXIOM from VG Elemental, UK). Element contents were calculated from the isotope ratios Ir^{191}/Ir^{193}, Ru^{99}/Ru^{101}, Pd^{105}/Pd^{106} and Pd^{105}/Pd^{108}, and Pt^{195}/Pt^{198}. Accuracy was checked against the WPR-1 certified reference material (Canmet, Canada certified values: Ir: 13.5 ng/g; Ru: 22 ng/g; Rh: 13.4 ng/g; Pd 235 ng/g; and Pt: 285 ng/g; this work: Ir: 16 ng/g; Ru: 20 ng/g; Pd 253 ng/g; and Pt: 280 ng/g) and the interlaboratory reference material ODP-serpentinite 147–895D-10W (Puchelt et al., 1996). Detection limits are 0.05 ng/g Ir, 0.1 ng/g Ru, 0.4 ng/g Pd, and 0.4 ng/g Pt. Detection limits are mainly dependent on blanks of the NiS-fire assay, which are at the same level as the detection limits. To identify outliers caused by nugget effect from the used chemicals, the samples within one section were analyzed in random order. Single positive outliers were repeated.

To separate the part of an element not bound to the diffuse terrigenous component (mainly aeolian), the so-called "excess concentrations" of various elements (El*) were calculated, similar to Murray and Leinen (1993, 1996) and Schroeder et al. (1997). This method is based on the assumption that immobile elements such as Al, Ti, Zr, and Nb are introduced into marine sediments mainly by diffuse terrigenous input (e.g., aeolian dust). Therefore "excess concentrations" can be estimated by $El^* = El_{total} - [Ti_{sample}{}^* (El_{NASC}/Ti_{NASC})]$ taking into consideration the bulk concentration of the element (El_{total}), the Ti concentration of the sample (Ti_{sample}), the concentration of the element in NASC (North American Shale Composite) or in the PAAS (Post-Archaean Average Australian Shale) (El_{NASC}, El_{PAAS}), and the Ti concentration in NASC (Ti_{NASC}). Because the aeolian input in the Caribbean originates mainly from North America, data for the NASC (Gromet et al., 1984) were used instead of PAAS (Taylor and McLennan, 1985), except where no NASC data were available (e.g., for Cu and Zn).

The ratio of "excess" and bulk concentrations $R = El^*/El_{total}$ can be used as a measure for the amount of nondetrital components in the sediment. Accuracy of the estimates depends on the composition of the local terrestrial rocks, which were exposed to weathering, but variations in the average composition of the source rocks are relatively small.

3.4. Stable Isotopes

Carbon and oxygen isotope ratios in the carbonate fraction of finely ground bulk samples from selected sections (Los Dos Plebes, La Lajilla, and Coxquihui) were determined by means of an automated carbonate preparation system connected online to an isotope ratio mass spectrometer (MultiPrep and Optima, both from Micromass UK Ltd). The preparation line is based on a standard method by measuring isotope ratios in CO_2 released by reaction with 100% phosphoric acid. Samples were dissolved in individual vials to eliminate the risk of cross-contamination, a requirement crucial for accurate and precise isotope ratio measurements on samples as small as <10 μg of calcite. Reference CO_2, calibrated and certified by Messer Griesheim (Germany), was used from a pressure bottle. Instrumental precision was better than 0.008‰ for $\delta^{13}C$ and <0.015‰ for $\delta^{18}O$. Accuracy was checked in each of the analytical batches by running the carbonate standard NBS19. Results were in the range of the certified values within ±0.1‰ for $\delta^{13}C$ and ±0.15‰ for $\delta^{18}O$. Isotope values are reported relative to the Vienna Peedee belemnite (NIST, 1992) standard for both carbon and oxygen. For selected samples from Mimbral, $\delta^{34}S$ were measured using the procedure described in Berner et al. (2001).

4. HIGH-RESOLUTION GEOCHEMICAL RECORDS

4.1. Los Dos Plebes 1 (LDP1)

At the Los Dos Plebes 1 outcrop, ~75 cm of gray marls of the Mendez Formation are exposed with a 2-cm-thick siltstone at 35 cm above the base and a 2-cm-thick brown claystone at the top. The clay content increases towards the top of the section. Planktic foraminiferal assemblages in the Mendez marls contain *Plummerita hantkeninoides* and thus indicate a latest Maastrichtian Zone CF1 age. The siliciclastic deposit (unit 1–3) is nearly absent, except for a 1–2-cm-thick light gray calcareous limestone. This indicates that deposition occurred at the edge of a channel or levee area. Above the thin limestone, dark gray claystones characterize the basal 5 cm of the Velasco Formation and grade into 1.5 m of gray shales and marls containing early Danian zone Pla assemblages (*P. eugubina*, Fig. 2).

PGE contents are generally low throughout the section (Fig. 2; Table 1). A small Ir anomaly and the highest PGE contents (0.32 ng/g Ir, 0.21 ng/g Ru, 0.6 ng/g Pt, and 1.2 ng/g Pd) are observed in the dark claystone (zone Pla) above the thin sandy limestone (Lindenmaier et al., 1999). A second small Pt (0.5 ng/g) and Pd (0.4 ng/g) enrichment, but without significant increase in Ir, is present in the marls between 35 to 45 cm below the K/T boundary (Fig. 2, Table 1). This Pt-Pd enrichment coincides with the occurrence of zeolites, which are typical products of glass alteration. In the thin limestone the concentrations of all trace elements decrease due to dilution by carbonate, whereas in the claystone above they return to pre K/T values. Within the first 40 cm of the early Danian claystone and shale, Ba, Zn, and Zr content gradually increase, whereas Sr gradually decreases (Fig. 2). The extremely low C and O isotope values (up to −6.3‰ for $\delta^{13}C$ and −12.5‰ for $\delta^{18}O$) (Fig. 2) suggest a strong diagenetic overprint (Schrag et al., 1995). Nevertheless, the record displays some general trends. From 60 cm to 20 cm below the K/T boundary, $\delta^{18}O$ and $\delta^{13}C$ remain nearly constant (~ −8‰ and ~ −6.5‰ respectively), followed by a steady decrease in $\delta^{18}O$ to −12‰ and $\delta^{13}C$ to −3.6‰. At the K/T boundary $\delta^{18}O$ increases to −9‰ and $\delta^{13}C$ decreases to −6.4‰. Above the K/T boundary, early Danian $\delta^{18}O$ and $\delta^{13}C$-values are ~2‰ lower than the late Maastrichtian values.

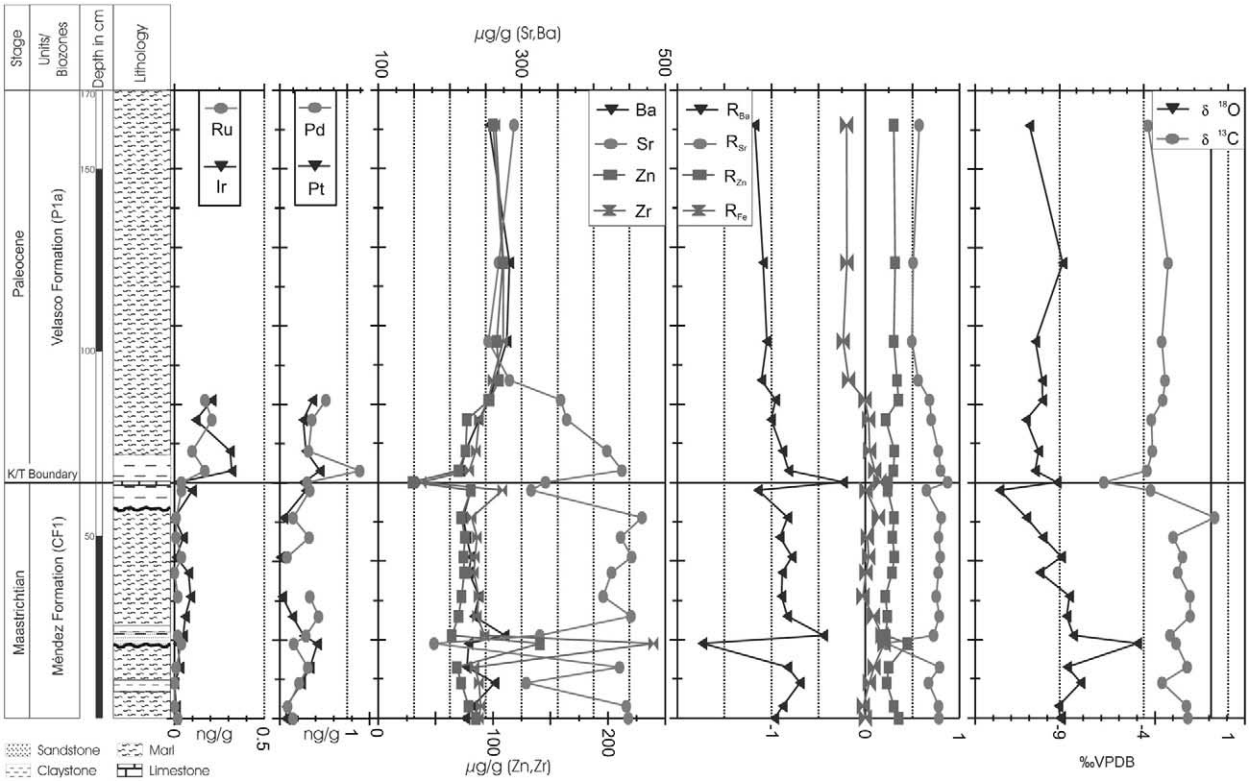

Fig. 2. Litholog, PGE data, trace element contents, excess ratios, and $\delta^{13}C$ and $\delta^{18}O$ isotope ratios across the K/T section of Los Dos Plebes (PGE in ng/g, trace elements in $\mu g/g$). The "excess" ratio $R = El^*/El_{total}$ with $El^* = El_{total} - [Ti_{sample}*(El_{NASC}/Ti_{NASC})]$ is a measure for the amount of nondetrital components in the sediment (Murray and Leinen, 1996). The excess ratios are discussed in section 7 of the text.

4.2. Loma Cerca

At Loma Cerca a 3.5-m-thick siliciclastic deposit, including a thin spherule unit 1 at the base, overlies an erosional surface of the Mendez marl formation. Over 15 m of Mendez marls are exposed. At 6 m and 10 m below the siliciclastic deposit are two distinct 1-m and 0.25-m-thick spherule layers, respectively (Fig. 3). Biostratigraphic analysis indicates the base of the latest Maastrichtian *P. hantkeninoides* Zone (CF1) ~1 m below the lowermost spherule layer. Based on the average sedimentation rate at this section, the age of the lowest spherule layer was estimated at 270 ± 30 kyr above the K/T boundary (Stinnesbeck et al., 2001; Keller et al., 2002a, 2003). The overlying spherule layer and the unit 1 spherules are interpreted as reworked sediments based on the presence of shallow water foraminifera and detritus.

Eighteen samples of spherule-rich sediments and the marls below, between and above the zone CF1 spherule layers were analyzed for PGEs. PGE contents remain low throughout the section and no Ir anomaly (Ir <0.17 ng/g) is associated with any of the spherule layers or marls (Fig. 3). An isolated enrichment of Pd (2.7 ng/g Pd) at ~6.5 m below the base of the siliciclastic deposit suggests alteration or hydrogenetic precipitation from the water column. A minor increase in Ir (0.17 ng/g) and Pd (3 ng/g) is only recognized at the top of the marl sequence at the erosive contact between the marls and overlying siliciclastic deposit.

The major and trace element composition in the marls remains nearly constant (e.g., MgO, Al_2O_3, SiO_2, CaO, Fe_2O_3, Ba, Sr, Zn, Zr, Table 1, Fig. 3). The slight variations reflect mainly fluctuations in the amount of terrigenous components as reflected by the element contents (Table 1). The spherule layer at 6.5 m below the siliciclastic deposit is characterized by a strong increase in Zr, which is mainly bound to the detrital component, a slight increase in Zn, a local enrichment in Ba, and low Sr content. The main variations in the trace element distribution occur in the spherule layer at 6.5 m below the siliciclastic deposit (Fig. 3), where Ba and Zr increase and Sr decreases significantly. The bulk chemistry of the spherule layer at 9 m below the siliciclastic deposit shows no significant contrast to the surrounding marls.

Stable $\delta^{13}C$ isotope values of bulk rock samples are rather uniform (around −1‰) with significantly more negative values of −2‰ to −3.5‰ restricted to the spherule-rich layers (Stinnesbeck et al., 2001). The markedly negative $\delta^{18}O$ values (around −8‰) indicate strong diagenetic alteration and recrystallization in the presence of meteoric water (Schrag et al., l995; Stüben et al., 2003). The uniform $\delta^{13}C$ values in the marl section suggest normal pelagic deposition and the absence of significant reworking. In the spherule layers of unit 1, $\delta^{13}C$ values are systematically lower and more variable than in the marls, probably due to a stronger diagenetic overprint and higher amounts of reworked and redeposited sediment (Fig. 3).

Table 1. Variation range (min, max), lower quartile Q_1 (25%), median (50%), and upper quartile Q_3 (75%) values for major element, trace element, and PGE data for the K/T sections at Bochil, El Peñon, EL Mulato, La Lajilla, Los Dos Plebes, Coxquihui, Loma Cerca; and Mimbral.[a]

		MgO	Al_2O_3	SiO_2	CaO	K_2O	TiO_2	Fe_2O_3	V	Cr	Ni	Cu	Zn	Ga	Rb	Sr	Y	Zr	Nb	Ba	La	Ce	Ir	Pt	Pd
		wt%							μg/g							μg/g							ng/g		
Bochil $n = 15$	min	n.d.	n.d.	n.d.	32.2	0.57	0.00	0.14	n.d.	n.d.	n.d.	7	7	<2	<1	183	<2	10	<2	39	<5	<5	0.24	0.47	0.82
	Q1	n.d.	n.d.	n.d.	36.1	0.94	0.07	0.62	n.d.	n.d.	n.d.	12	12	<2	7	211	2	18	<2	81	<5	8	0.29	1.01	1.29
	med	n.d.	n.d.	n.d.	42.0	1.51	0.12	1.32	n.d.	n.d.	n.d.	23	16	3	11	253	5	23	<2	129	6	11	0.44	1.25	1.71
	Q3	n.d.	n.d.	n.d.	44.4	1.69	0.17	1.93	n.d.	n.d.	n.d.	26	34	4	19	352	7	35	<2	246	10	18	0.55	1.88	2.02
	max	n.d.	n.d.	n.d.	50.4	2.09	0.27	3.52	n.d.	n.d.	n.d.	37	47	8	37	459	11	47	2	1131	15	33	1.21	2.88	3.19
Peñon $n = 15$	min	n.d.	n.d.	n.d.	16.8	1.57	0.31	2.24	n.d.	n.d.	<5	16	35	4	31	389	12	59	<2	183	6	20	<0.05	0.46	0.56
	Q1	n.d.	n.d.	n.d.	18.2	1.75	0.34	2.93	n.d.	n.d.	12	18	48	6	37	479	13	68	3	215	13	32	0.05	0.49	0.70
	med	n.d.	n.d.	n.d.	20.6	1.91	0.36	3.32	n.d.	n.d.	16	20	58	9	59	496	13	77	3	278	16	37	0.08	0.59	0.80
	Q3	n.d.	n.d.	n.d.	27.7	2.22	0.40	3.55	n.d.	n.d.	17	22	65	10	61	565	13	80	4	389	24	43	0.10	0.77	0.87
	max	n.d.	n.d.	n.d.	35.2	2.64	0.43	5.17	n.d.	n.d.	22	24	72	12	69	664	14	88	5	707	27	67	0.16	0.83	1.22
El Mulato $n = 20$	min	0.82	4.96	23.4	10.7	0.53	0.19	1.35	n.d.	n.d.	6	9	<5	3	<1	12	<2	<2	<5	<5	13	0.07	0.62	<0.4	
	Q1	1.90	9.18	39.9	13.3	1.33	0.36	3.06	n.d.	n.d.	12	18	45	9	41	399	14	79	<2	139	16	43	0.13	1.10	1.16
	med	2.45	11.9	44.8	15.2	2.18	0.52	4.13	n.d.	n.d.	17	24	78	12	70	510	18	89	5	164	18	52	0.23	1.35	1.55
	Q3	2.61	13.1	47.6	22.2	2.45	0.57	4.92	n.d.	n.d.	20	34	99	14	86	648	23	109	6	213	30	67	0.39	1.51	1.87
	max	2.97	13.8	54.0	34.7	3.07	0.69	5.45	n.d.	n.d.	27	82	115	16	97	1393	159	136	17	1867	485	194	0.99	2.99	2.36
LaLajilla $n = 22$	min	0.27	6.29	1.44	0.54	13.09	0.50	0.09	36	30	12	11	28	4	15	311	11	50	<2	40	<5	50	<0.05	<0.2	<0.4
	Q1	0.28	7.30	1.52	0.66	14.64	1.39	0.09	81	41	23	15	46	7	33	353	13	96	3	134	13	68	<0.05	<0.2	<0.4
	med	0.41	9.98	2.57	1.26	18.86	1.64	0.11	114	54	36	23	73	11	61	413	16	108	5	196	18	85	0.05	0.28	<0.4
	Q3	0.52	11.2	4.13	1.82	22.54	2.46	0.14	125	57	39	27	89	13	72	514	18	131	5	896	24	105	0.11	0.35	0.45
	max	0.70	13.5	15.0	2.59	40.56	2.80	0.15	151	67	48	113	114	15	87	578	26	286	7	2867	36	137	0.24	0.79	0.80
LaSierrita	min															178	9	38	<2	147	8	41	<0.05	<0.2	<0.4
	Q1															308	15	85	4	224	16	76	<0.05	<0.2	<0.4
	med															389	16	88	5	231	20	85	<0.05	<0.2	<0.4
	Q3															440	17	99	5	255	23	99	0.09	0.38	0.45
	max															468	19	240	7	283	30	110	0.32	0.60	1.19
Los Dos Plebes $n = 22$	min	0.20	5.74	2.12	0.90	11.51	0.45	0.06	29	28	16	13	30	6	27										
	Q1	0.45	10.6	4.31	1.26	15.02	0.66	0.10	120	52	30	18	73	8	67										
	med	0.48	11.2	4.58	1.81	19.32	0.89	0.12	126	56	31	20	76	11	72										
	Q3	0.55	11.7	4.77	1.88	19.81	0.92	0.14	145	67	32	23	94	13	79										
	max	0.68	12.8	7.64	2.14	43.75	4.49	0.44	168	83	45	32	141	15	90										
Coxquihui $n = 24$	min	0.71	5.13	15.4	12.6	0.87	0.19	0.73	n.d.	n.d.	n.d.	13	12	2	7	231	8	39	<2	29	8	25	0.06	0.48	0.91
	Q1	0.81	5.35	15.7	13.0	0.91	0.21	1.06	n.d.	n.d.	n.d.	27	45	7	50	288	14	69	3	137	14	30	0.10	0.79	1.23
	med	1.53	9.39	35.9	19.4	1.80	0.41	3.77	n.d.	n.d.	n.d.	33	59	9	61	347	15	83	4	170	17	32	0.13	0.94	1.91
	Q3	1.93	11.6	41.3	25.0	2.26	0.50	4.41	n.d.	n.d.	n.d.	54	73	11	70	390	17	93	5	195	20	37	0.17	1.14	2.18
	max	2.54	12.8	49.6	41.1	2.52	0.59	4.80	n.d.	n.d.	n.d.	93	95	13	82	1268	20	147	6	227	26	60	0.48	1.74	2.93
Loma Cerca $n = 27$	min	1.31	9.38	22.5	7.78	0.80	0.33	3.29	70	43	20	11	39	2	26	285	13	67	3	128	<5	28	<0.05	<0.2	0.53
	Q1	1.95	10.4	36.6	17.8	1.90	0.45	4.30	102	71	22	17	73	10	65	436	15	88	4	180	17	32	0.05	<0.2	1.06
	med	2.08	11.0	42.4	19.5	2.04	0.48	4.43	111	74	24	19	75	13	73	475	16	90	5	199	19	38	0.07	0.31	1.27
	Q3	2.13	11.5	44.1	21.3	2.15	0.55	4.85	122	77	27	21	81	16	76	497	16	94	5	223	24	44	<0.05	0.35	0.53
	max	2.35	13.0	48.9	31.7	2.77	1.00	9.44	131	83	40	37	101	31	103	541	19	225	7	476	31	54	0.10	0.75	4.49
Mimbral $n = 53$	min	0.53	6.47	21.8	13.0	0.62	0.22	1.58	<20	25	13	8	32	n.d.	16	366	11	121	8	80	<5	10	n.d.	n.d.	n.d.
	Q1	1.82	9.64	39.7	17.0	1.62	0.43	3.58	89	68	25	21	74	n.d.	61	400	14	137	14	184	12	32	n.d.	n.d.	n.d.
	med	2.04	10.6	43.9	18.4	1.80	0.47	3.93	96	71	28	23	82	n.d.	67	448	15	139	15	230	17	39	n.d.	n.d.	n.d.
	Q3	2.22	11.2	45.2	20.9	1.91	0.50	4.21	112	74	30	25	87	n.d.	71	471	16	141	16	272	22	43	n.d.	n.d.	n.d.
	max	2.32	12.1	49.5	32.1	2.25	0.51	4.58	131	91	44	31	106	n.d.	83	526	22	201	20	422	30	54	n.d.	n.d.	n.d.

n.d. = not detected.

[a] Median, Q_1, and Q_3 are robust parameters, which are characteristic for the composition of the marls within the different sections. Minimum and maximum values are the extrema at the K/T boundary, or in thin intercalated layers of sedimentary or volcanoclastic origin. The complete data set is available on request from the Institute of Mineralogy and Geochemistry.

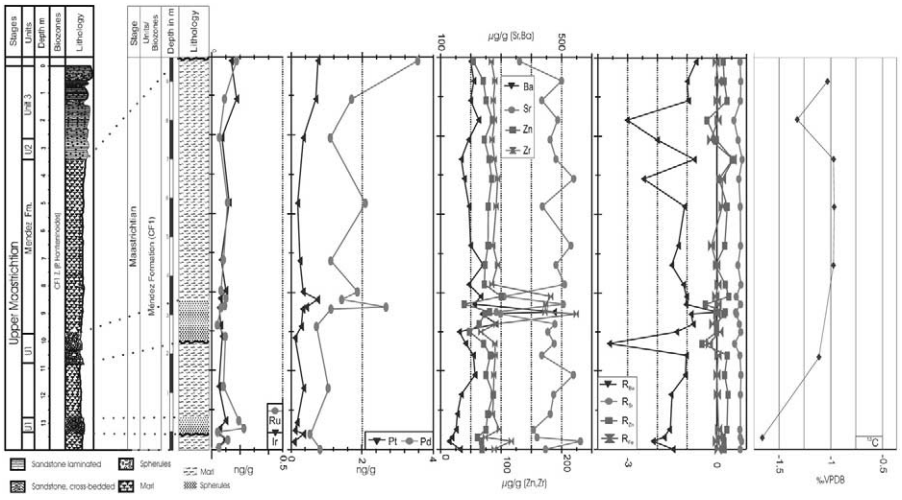

Fig. 3. Litholog, PGE data, trace element contents, excess ratios, and $\delta^{13}C$ isotope ratios across the K/T section of Loma Cerca (PGE in ng/g, trace elements in μg/g; $\delta^{13}C$ isotope ratios redrawn from Stinnesbeck et al., 2001). Left profile: complete section showing the position relative to the K/T boundary; right profile: close-up of the sampling interval.

4.3. El Peñon

The siliciclastic deposit of El Peñon varies in thickness from 8 m (at the classic El Peñon I outcrop) to less than 2 m over 200 m, probably as a result of channelized deposition (Keller et al., 1994; Stinnesbeck and Keller, 1996). No sediments overlying the siliciclastic deposit are present at El Peñon due to erosion. Mendez marls of the latest Maastrichtian Zone CF1 are exposed below the siliciclastic deposit and contain interlayered spherule-rich deposits. Our investigation focused on this marl interval and the interlayered spherule layers below the siliciclastic deposit of the El Peñon II outcrop (Fig. 4).

No distinct PGE anomalies are observed, and the trace elements (Zn, Zr, CaO, and TiO_2) vary around background values (Zn: ~60 μg/g; Zr: ~75 μg/g, Ba: ~300 μg/g), except for Ba, that is enriched at the base of unit 1 (700 μg/g) and shows a

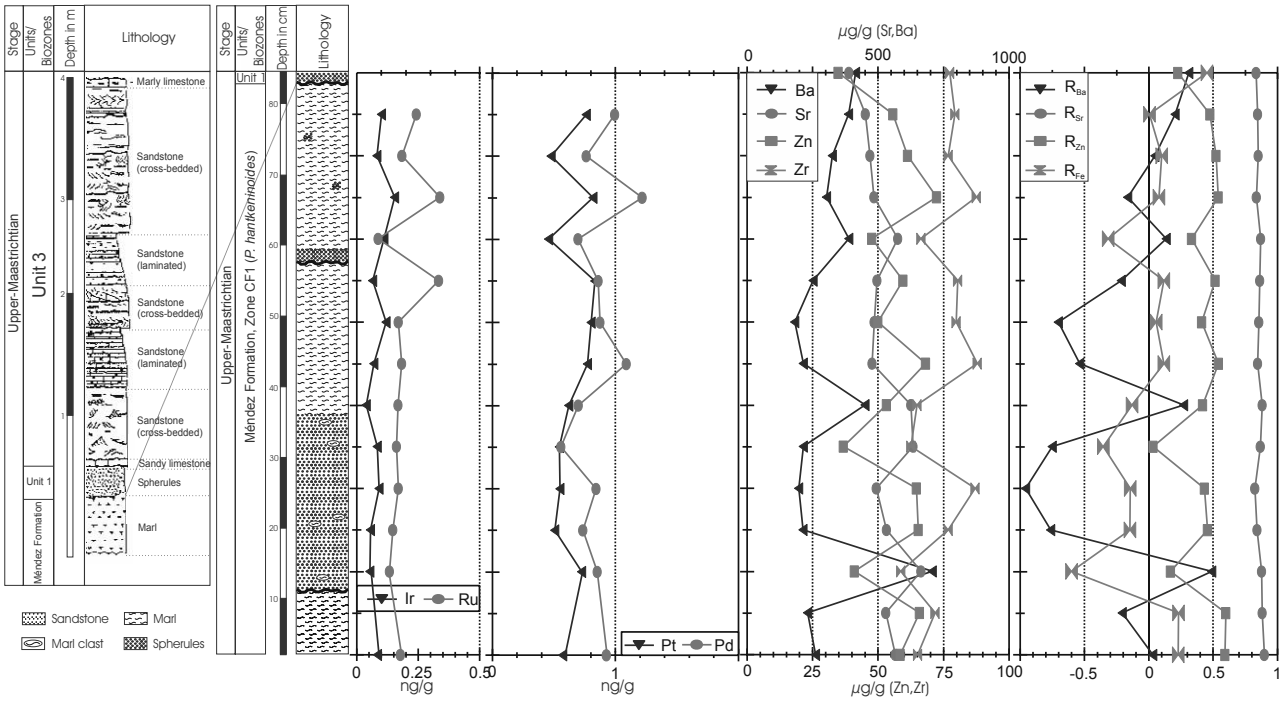

Fig. 4. Litholog, PGE data, trace element contents, and excess ratios across the K/T section of El Peñon (PGE in ng/g, trace elements in μg/g). Left profile: complete section showing the position relative to the K/T boundary; right profile: close-up of the sampling interval.

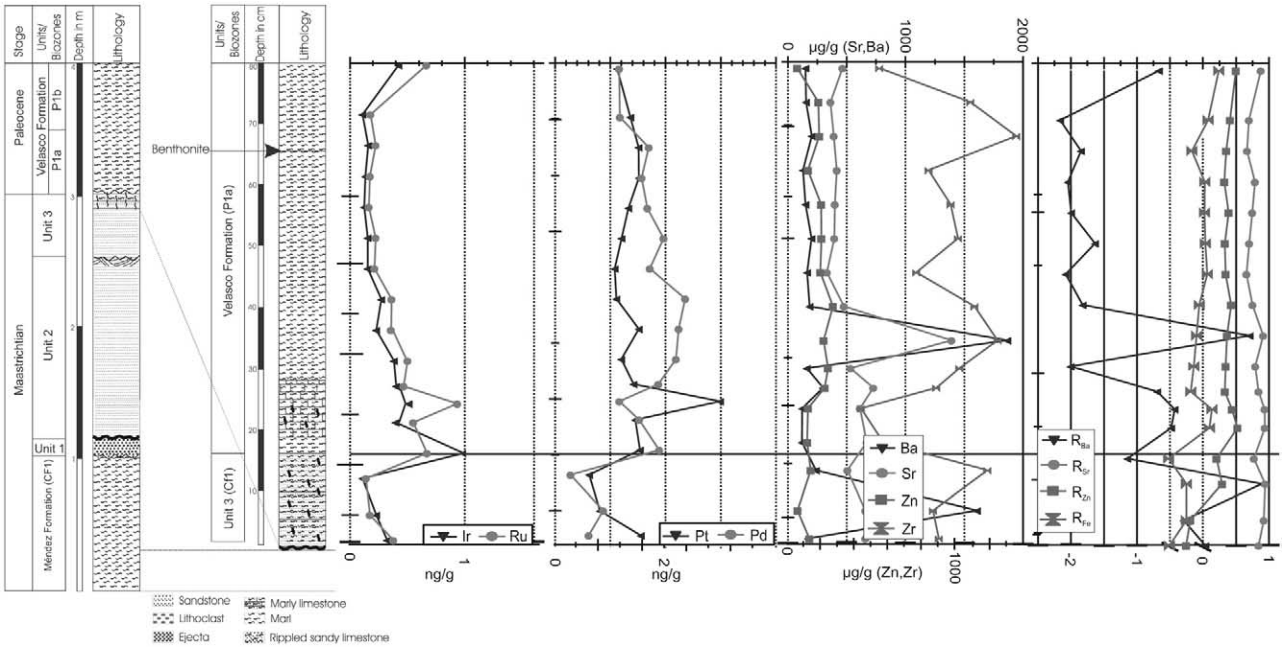

Fig. 5. Litholog, PGE data, trace element contents, and excess ratios across the K/T section of El Mulato (PGE in ng/g, trace elements in μg/g). Left profile: complete section showing the position relative to the K/T boundary; right profile: close-up of the sampling interval.

second anomaly at the top of unit 1. Strontium is well correlated with Ca (CaO), indicating that the major part of Sr is bound to carbonates (Fig. 4, Table 1).

4.4. El Mulato

The El Mulato section consists of a 2-m-thick siliciclastic deposit sandwiched between gray marls of the Maastrichtian Mendez Formation and gray shales of the Paleocene Velasco Formation (Fig. 5). ~20 m of the Mendez marls and 10 m of the Velasco shales are exposed at the El Mulato outcrop. López-Oliva and Keller (l996) reported the presence of a thin layer of latest Maastrichtian (CF1) Mendez marl overlying the siliciclastic deposit. This layer was not recognized during our recollection of the El Mulato section possibly due to the undulating contact and variable erosion. In the section analyzed, the first early Danian Zone P1a(1) planktic foraminiferal assemblage is present in a 3-cm-thick gray marl layer near the top of the siliciclastic deposit. This marl overlies a bioturbated and cross-bedded sandy limestone, which corresponds to the rippled sandy limestone described by Keller et al. (1994) and Stinnesbeck and Keller (1996). Above the gray marl is an 8-cm-thick resistant layer of gray marly limestone, which is bioturbated by *Chondrites*, *Thalassinoides*, *Teichichnus* and *Planolites*. A monotonous sequence of fissile gray marls of the Velasco Formation overlies this limestone layer and also contains diverse *P. eugubina* Zone (P1a) planktic foraminiferal associations. We sampled and analyzed a 1-m-thick section from the rippled sandy limestone across the K/T boundary into the marls of the Velasco Formation.

At Mulato a PGE anomaly is present in the 3-cm-thick gray marl layer of the early *P. eugubina* Zone (P1a), which overlies the bioturbated rippled sandy limestone. Iridium reaches 1 ng/g (higher than at Mimbral), Ru 0.7 ng/g, and Pt 1.5 (Fig. 5, Table 1). The highest Pt (3 ng/g) and Pd (2.4 ng/g) concentrations in the marls are slightly displaced (8 cm resp. 12 cm) towards the top. This PGE anomaly tails 20 cm into the overlying marly sediments. Trace and major elements show considerable variations. Fluctuations in the Zr concentrations reflect varying amounts of terrigenous components or ejecta. Barium shows two local enrichments 20 cm above and 20 cm below the Ir anomaly.

4.5. La Lajilla

At La Lajilla ~75 cm of gray marls of the Upper Maastrichtian Mendez Formation are exposed. The siliciclastic deposit consists of a relatively thin spherule layer (5 cm) and sandy limestone of unit 1 (SLL in Fig. 6) and a 1.3-m-thick unit 3; unit 2 is missing. This deposit overlies an erosional surface of the Mendez marl. Above unit 3 a 5–10-cm-thick layer of Maastrichtian marl was observed by López-Oliva and Keller (l996), followed above by 50 cm dark gray shales of the early Danian zone P1a of the Velasco Formation (Fig. 6). PGE values are close to or below detection limits in the Mendez marls and in the siliciclastic deposit, including the spherule-rich unit at the base. However, directly above a rippled sandy limestone is a small Ir-dominated PGE anomaly (0.24 ng/g Ir, 0.21 ng/g Ru, 0.44 ng/g Pt, and 0.52 ng/g Pd; Lindenmaier et al., 1999) (Fig. 6, Table 1). The Ir anomaly decreases upsection in the shales of the Velasco Formation returning to background values 20 cm above the maximum, whereas Pt and Pd values remain high, nearly at the same level as at the K/T-boundary (Fig. 6). Trace element contents remain at nearly constant levels throughout the section, with the exception of Ba, which shows a significant peak (2870 μg) ~40 cm below the K/T

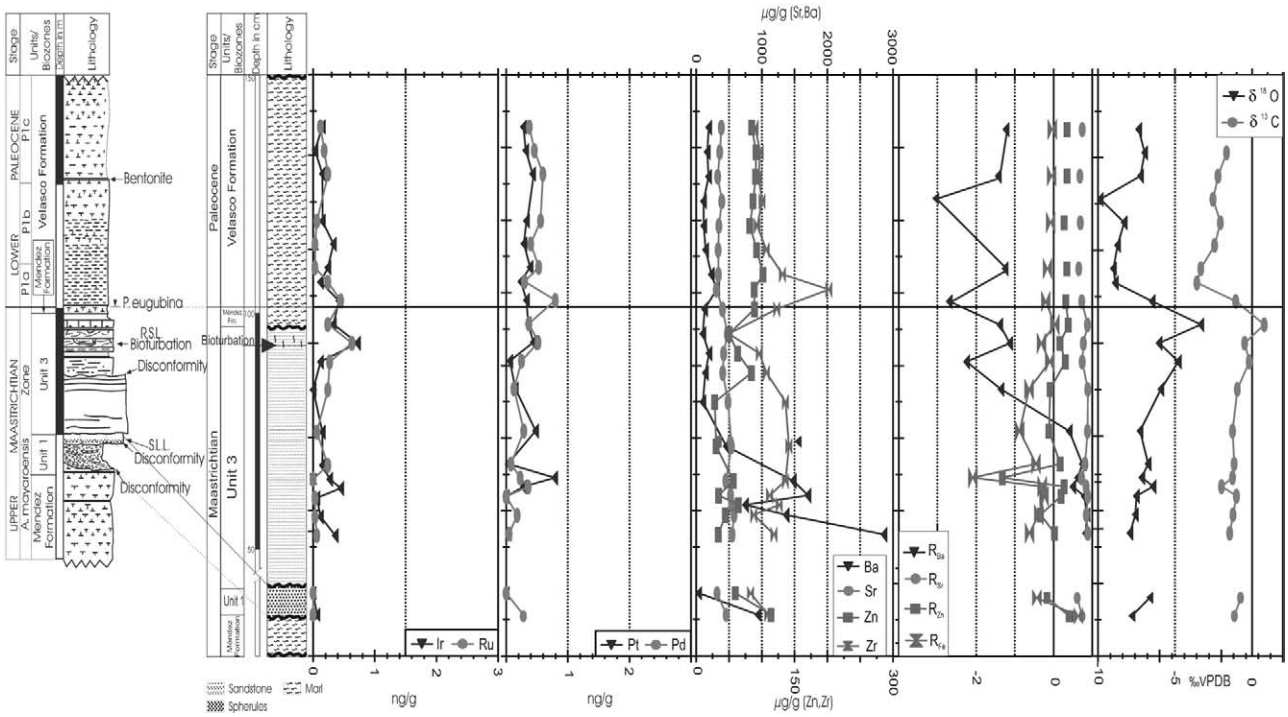

Fig. 6. Litholog, PGE data, trace element contents, excess ratios, and $\delta^{13}C$ and $\delta^{18}O$ isotope ratios across the K/T section of La Lajilla (PGE in ng/g, trace elements in $\mu g/g$). Left profile: complete section showing the position relative to the K/T boundary; right profile: close-up of the sampling interval.

boundary at the base of the sandy limestone (unit 3). Varying CaO contents correlate with decreasing Zr and TiO_2. Above the Ir anomaly, Zr shows a pronounced increase at the base of the Velasco formation, but within 10 cm returns to levels observed in unit 3.

Very negative $\delta^{18}O$ and $\delta^{13}C$ values indicate a strong diagenetic overprint at La Lajilla, similar to the Los Dos Plebes 1 section (Figs. 2, 6). Nevertheless, general trends can be observed. In the 65 cm below the K/T boundary, $\delta^{18}O$ values steadily increase from $-8‰$ to $-3.3‰$ and $\delta^{13}C$ increases from $-1.44‰$ to $0.8‰$. At the K/T boundary, identified by the first appearance of Danian species, a strong negative shift in ^{13}C and ^{18}O isotopes is observed from 0 to $-3.5‰$ in $\delta^{13}C$ and from $-4‰$ to $-9‰$ in $\delta^{18}O$. Above the K/T boundary $\delta^{13}C$ values recover to $-1.6‰$ and $\delta^{18}O$ values recover to $-7‰$.

4.6. Mimbral

At Mimbral, a channelized siliciclastic deposit can be followed along the outcrop for more than 60 m. In the center of the channel, the deposit is 3 m thick and peters out to 20 cm at the edges (Keller et al., 1994). This deposit overlies an erosional surface on the gray marls of the Mendez Formation. Above the siliciclastic deposit are the dark shales of the Velasco Formation (Fig. 7). We analyzed a section at the edge of the channel known as Mimbral II (Keller et al., 1994), which includes 30 cm of Mendez marls, a 20-cm-thick sandy limestone at the top of unit 3, and 200 cm of the Velasco Formation shales. A small Ir anomaly of 0.8 ng/g was reported by Smit et al. (1992) in the center of the channel. This Ir anomaly reaches a maximum in the basal Velasco shales of the early Danian zone Pla, just above the rippled sandy limestone that marks the top of the siliciclastic deposit (Stinnesbeck et al., 1993; Keller et al., 1994, Fig. 7). Major and trace element concentrations also show the comparatively strongest variations in this layer. A more carbonate-rich layer of the Velasco Formation is accompanied by a sharp decrease in Zn, Cr, Ni, and V and increase in Ba (Fig. 7, Table 1).

4.7. Coxquihui

The siliciclastic deposit appears to be absent at Coxquihui. A 1-cm-thick spherule layers is present at or near the K/T boundary, which is characterized by a hiatus that spans from the lower *P. eugubina* Zone (P1a(1)) to the upper part of the latest Maastrichtian *Plummerita hantkeninoides* Zone (CF1, Stinnesbeck et al., 2002). ~20 cm above the K/T boundary is a 60-cm-thick spherule layer within the early Danian *P. eugubina* (P1a) Zone (Fig. 8). No significant PGE anomalies are observed in the spherule layers or the Maastrichtian marls. However, minor enrichments of Ir (0.22 ng/g) and Pt (up to 1.45 ng/g) are present in the marls directly above the paleontologically defined K/T boundary above the 1-cm-thick spherule layer. Values decrease to background levels in the 15 cm marl upsection. The nonchondritic Ir/Pt ratio of 0.15 of this Ir anomaly is suggestive of a nonimpact origin and not necessarily linked to the K/T-boundary event.

A second small Ir anomaly is present in the early Danian zone P1a at the base of the marls directly overlying the 60-cm-thick upper spherule layer and tails upsection for ~15 cm (Fig.

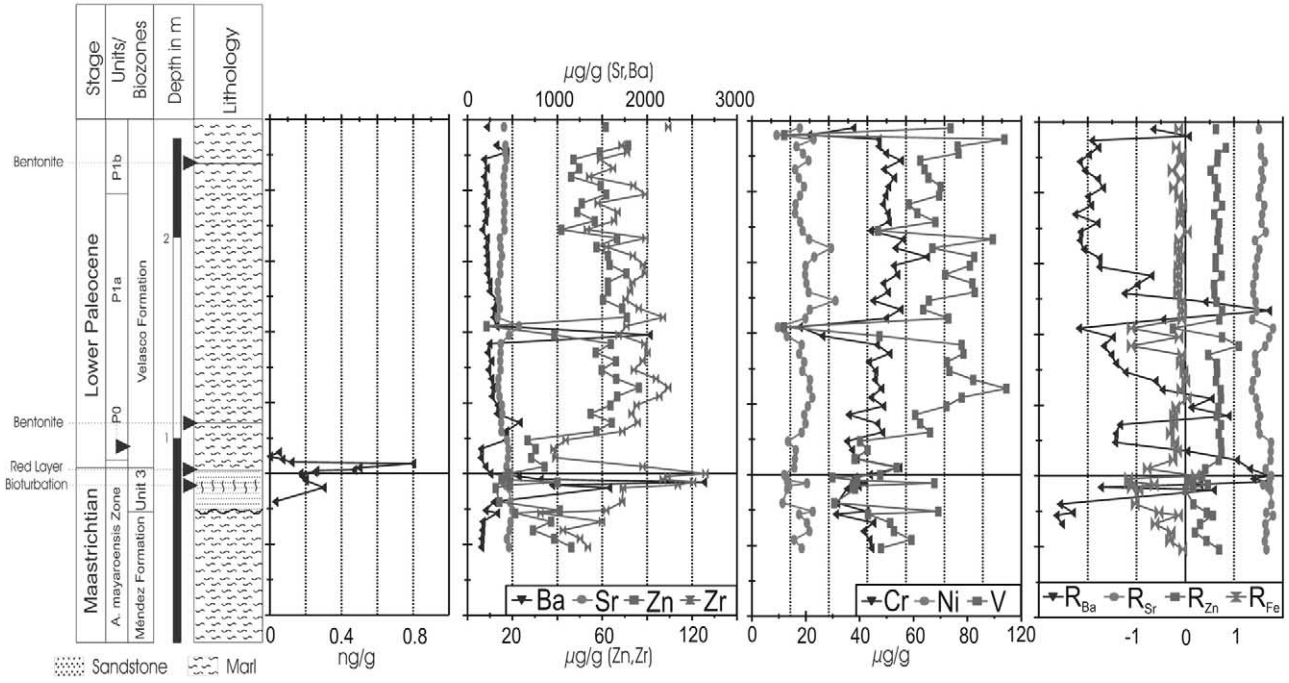

Fig. 7. Litholog, Ir data, trace element contents, and excess ratios across the K/T section of Mimbral. (PGE in ng/g, trace elements in μg/g, Ir data from Keller et al., 1994).

8, Table 1). The maximum Ir concentration of 0.5 ng/g is accompanied by the highest Pt content (1.7 ng/g) and minor enrichments of Ru and Pd. This nearly chondritic Pt/Ir ratio exceeds the local background by ~0.4 ng/g for Ir and 0.9 ng/g for Pt. If the average background value (0.15 ng/g for Ir and 0.94 ng/g for Pt) is subtracted, an excess Ir/Pt ratio of 0.44 is obtained, which is practically identical to the chondritic ratio of 0.45 (McDonough and Sun, 1995). Palladium shows a stronger

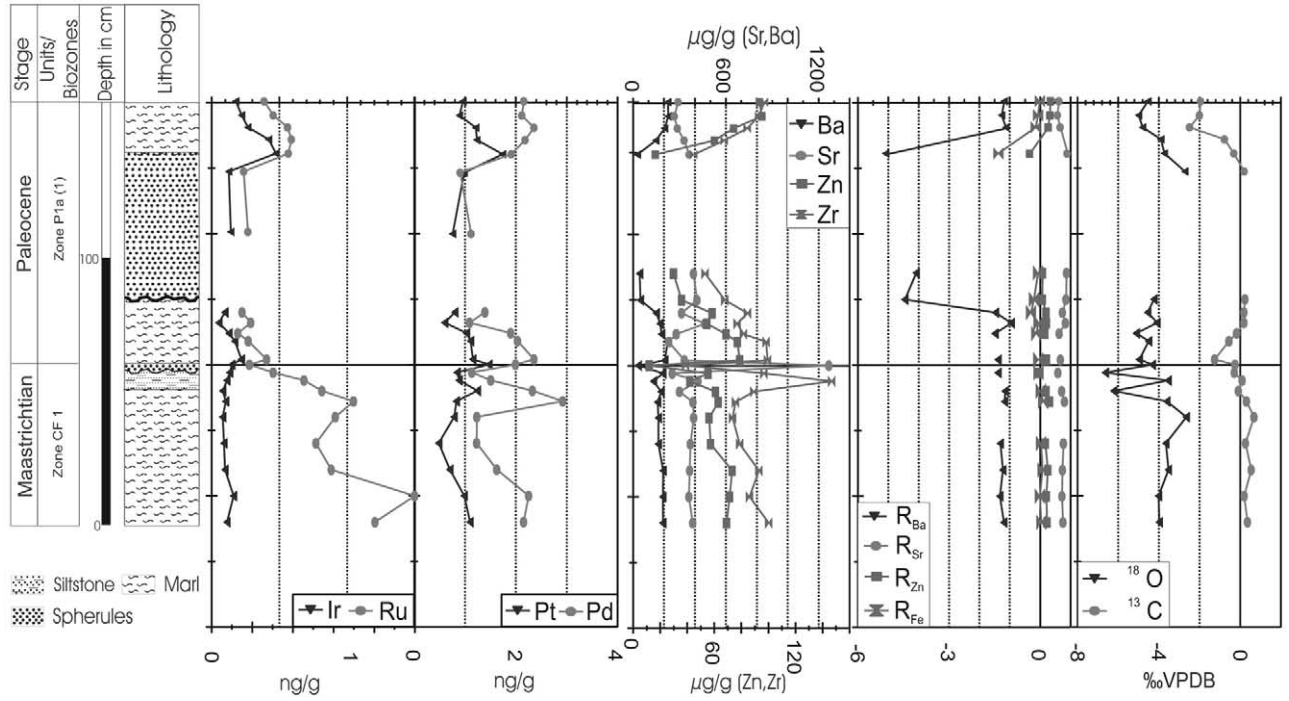

Fig. 8. Litholog, PGE data, trace element contents, excess ratios, and $\delta^{13}C$ and $\delta^{18}O$ isotope ratios across the K/T section of Coxquihui (PGE in ng/g, trace elements in μg/g).

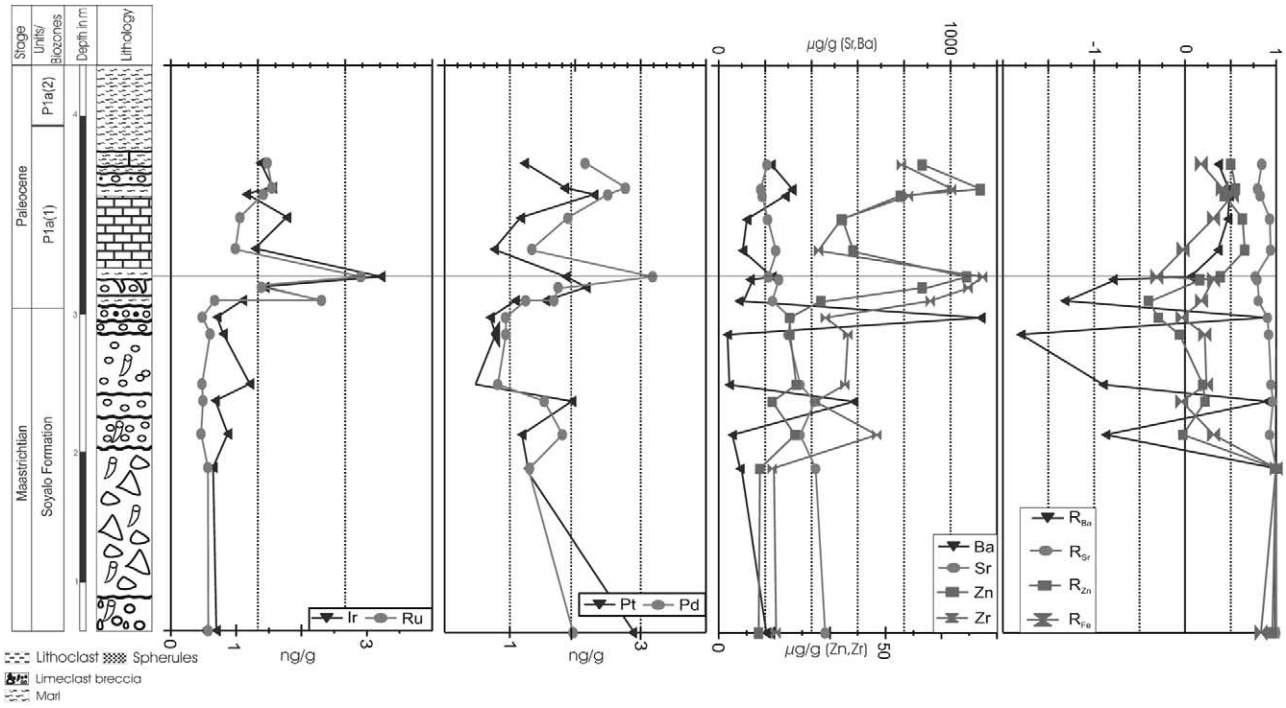

Fig. 9. Litholog, PGE data, trace element contents, and excess ratios across the K/T section of Bochil (PGE in ng/g, trace elements in μg/g).

tailing to the top of the section than the other PGE. Trace and major elements show strong variations throughout the section (Fig. 8, Table 1). A few centimeters below the lower PGE anomaly at the K/T transition, Zr and Sr are enriched from 70 and 150 μg/g to 400 and 1200 μg/g respectively, whereas Ba and Zn are slightly depleted.

$\delta^{18}O$ values vary between $-2.5‰$ and $-5.1‰$ and $\delta^{13}C$ between $0.5‰$ and $-2.5‰$, except for two outliers ($-6.6‰$ and $-6.2‰$) with strong diagenetic overprint (Fig. 8). During the late Maastrichtian zone CF1 there is a steady increase in $\delta^{18}O$ from $-4‰$ to $-3‰$, whereas $\delta^{13}C$ remains nearly constant. Fifteen cm below the paleontological K/T boundary, $\delta^{18}O$ and $\delta^{13}C$ values decrease reaching $-6‰$ and $-1.8‰$, respectively. Above the K/T boundary, $\delta^{18}O$ and $\delta^{13}C$ values recover to $-4‰$ and $0.2‰$ respectively, with maxima at the top of the upper spherule layer. At 80 cm above the K/T boundary, isotope ratios decrease again (Fig. 8).

4.8. Bochil, Southern Mexico

At Bochil, a 1-m-thick limestone microconglomerate with spherule debris disconformably overlies a limestone breccia with abundant Campanian-Maastrichtian shallow water carbonate platfom debris (e.g., rudists, large benthic foraminifera) and underlies shales, marls, and marly limestones of the Danian Soyalo Formation. The first early Danian zone Pla(l) assemblage is found in a 3-cm-thick layer of white marl that directly overlies the top of the microconglomerate (Fig. 9). The presence of Cheto smectite coincides with the presence of rare but very well preserved spherules and persists through the marls and shales of subzone P1a(1) and part of subzone P1a(2) (Keller et al., 2003). Background concentrations of 0.2 to 0.4 ng/g Ir are present throughout the section and are thus much higher than values measured in sections of NE Mexico. A sharp PGE anomaly with concentrations up to 1.2 ng/g Ir, 1.1 ng/g Ru, 2.2 ng/g Pt, and 3.2 ng/g Pd is observed in marls of the early Danian subzone P1a(1), ~8 cm above the microconglomerate with spherules and directly overlying a bioturbated marl layer. At 20 cm above this anomaly is a second PGE anomaly. Platinum reaches 2.3 ng/g and Pd 2.8 ng/g whereas Ir and Ru are not enriched (Fig. 9, Table 1). The microconglomerate and breccia below the lower PGE anomaly are characterized by varying amounts of Ba, Zn, and Zr and Sr. In the marly limestones overlying the lower PGE anomaly, Ba, Sr, Zn, and Zr remain nearly constant. At both PGE anomalies Sr and Ba contents remain nearly constant, whereas Zr and Zn are enriched by a factor of 2 to 3 (Fig. 9). ~10 cm below the Ir-dominated PGE anomaly, an isolated Ba anomaly is observed that is not accompanied by other trace elements.

5. STATISTICAL DATA EVALUATION

The abundance of trace elements in sediments is controlled by various factors, including terrigenous influx, biogenic flux, hydrothermal input and sedimentation rates, weathering, and diagenesis (Murray and Leinen, 1993; Richter and Liang, 1993; Schroeder et al., 1997; Andreozzi et al., 1997; Bach and Irber, 1998; Hannigan and Basu, 1998). The complex interaction of these different processes strongly overprints primary paleooceanographic signals and frequently enhances a simplistic straightforward interpretation. Multivariate statistical methods are used here to distinguish between the complex effects and interactions of different geochemical factors and processes.

5.1. Cluster Analysis

R-mode hierarchical cluster analysis, using the Pearson correlation coefficients as similarity measure and Wards agglomeration method (Rock, 1988) and principal component analysis in combination with Varimax factor rotation (Rock, 1988) as provided by STATISTICA V5.1 were applied to the geochemical data of each section. These methods reveal similarities and dissimilarities in the behavior of the different elements between sections. For the Los Dos Plebes and El Mulato sections, the results of hierarchical cluster analysis are presented in Figure 10. Generalizing for all sections, three major groups of elements can be distinguished:

The first group characterizes the authochtonous components of the basin. In this group, Ca, Mn, and LOI always cluster. Elements that are mainly (co-)precipitated from the water column or linked to bioproductivity are assigned to this group, as well as some elements that may be bound to clay minerals. Diagenetic calcite is also included in this group. This group will be referred as the carbonate/marl group. The second and third groups characterize the allochtonous components of the basin. In these groups, elements of terrigenous origin are clustered, which are either bound to sheet silicates, mainly to clay minerals, (terrigenous clay group: Al, Ga) or which are bound to detrital minerals (residual group: Zr, Nb, SiO_2). The clay mineral group includes detrital sheet silicates, as well as clay minerals formed from glass weathering. The different sections investigated are characterized by varying element associations in these two groups, and variations in amounts of terrigenous clays and residual minerals.

Strontium clusters within the group of sedimentary carbonates at Los Dos Plebes (Fig. 10), El Peñon, Coxquihui, and Bochil, indicating that in these sections the major part of Sr is bound to (biogenic) carbonates. Ba clusters with Zr and Nb, indicating that Ba is mainly bound to residual phases (e.g., at Los Dos Plebes, Fig. 10). Because in R-mode cluster analysis a variable can only be assigned to one cluster exclusively, a part of Ba may also be present in the biogenic fraction. The PGEs cluster together within one of the three major groups. At Los Dos Plebes, Ir, Pt, and Pd form a subgroup, which is loosely associated with the carbonate/marl group, whereas at El Peñon, all PGEs are assigned to the residual group. At Coxquihui, El Mulato (Fig. 10), and La Lajilla, Pd is separated from the other PGE and is always linked to terrigenous clays, whereas Ir, Pt, and Ru are either associated with the autochtonous marl group or the residual group.

5.2. Factor Analysis

To obtain more detailed information, factor analysis was applied to bulk chemical compositions. Factor analysis is more selective than hierarchical cluster analysis. Factors were extracted for all of the sections investigated. Factor 1 and 2 loadings for major and trace elements of selected sections (El Mulato, Coxquihui, Bochil, and Los Dos Plebes) are presented in Figure 11.

In the data sets of all sections, except for Bochil, one factor reflects the opposite trend between the detrital continental input and biogenic/authigenic sedimentation. This factor is characterized by high loadings for elements typically bound to minerals of terrigenous origin (e.g., Al, Si, Ti, Ga, Rb, Zr), and high but opposite loadings for the carbonate component (Ca). This factor includes the major elements Al, Si, and Ca, which account for most of the elemental contents. Due to the closure effect (summing up to 100%), which has to be taken into consideration for these elements, Al, Si on the one hand, and Ca on the other hand, are not separated into different factors but occur with opposite signs within the same factor. In most sections Ca is associated with Mn. In most cases this factor accounts for the major part of the variance (factor 1).

At La Lajilla, El Mulato, El Peñon, and Los Dos Plebes, high loadings for elements representing the clay/detrital fraction and those representing the carbonate fraction are included with opposite signs to one or two detrital and one or two clay-dominated factors. The separation of Ti and Zr with high factor loadings in different detrital factors is mainly due to the occurrence of two groups within one section showing different characteristic Zr/Ti ratios (Fig. 12). This is observed for the sections at Mimbral, Loma Cerca, El Mulato, and La Lajilla, whereas strictly linear correlations of Ti and Zr are observed for the sections at Los Dos Plebes, Coxquihui, and Bochil (Fig. 12). The separation into two groups with different characteristic Ti-Zr ratios within each of the sections (Mimbral, Loma Cerca, El Mulato, and La Lajilla) may indicate changing sources for detrital components in the sediments.

In most sections, PGEs are associated with a clay factor (Ir at Loma Cerca and Bochil) or with a detrital factor (Ir and Pt at Coxquihui and Ir at La Peñon). A separate PGE factor, characterizing the PGE anomaly, is obtained for La Lajilla (Ir, Ru), Los Dos Plebes (Ir, Pd, Pt), and El Mulato (Ir, Ru, Pt). The clay/detrital (positive loadings) and carbonate (negative loadings) factor of the sections at La Lajilla, El Mulato, and Coxquihui includes high positive loadings of Pd.

At El Peñon, where no Ir anomaly was observed, factor 2 is characterized by high loadings of Cu, Ru, Pt, and Pd. This may indicate possible reduction processes. Iridium is separated from other PGEs, but associated with the typical detrital component Nb. Assuming an approximately constant flux of cosmic matter, background Ir is controlled by varying dilution at changing sedimentation rates (Bruns et al., 1996). Thus the strong correlation of Ir and the detrital controlled Nb ($r = 0.835$) may reflect changing sedimentation rates during the deposition of the sedimentary column.

Platinum is closely correlated to Ba at Loma Cerca ($r = 0.70$) and at La Lajilla ($r = 0.91$). Besides detrital sedimentation and hydrothermal activity, precipitation of $BaSO_4$ can occur within the microenvironment of decaying biologic debris (McManus et al., 1999). Since at Loma Cerca, Ba is not linked to any of the clay/detrital factors, this mechanism seems to be probable and Pt may have been absorbed on biologic debris.

At Coxquihui, Los Dos Plebes, and Bochil Sr and at El Peñon Ba are associated with the carbonate group of the clay/carbonate factor, indicating that at these locations the major part of Sr and at El Peñon also of Ba is of biogenic origin.

6. RECONSTRUCTION OF THE IMPACT EVENTS AND RELATIONSHIP TO THE K/T BOUNDARY

Based on the extremely high Ir contents of meteorites, as compared to average earth crust (10,000 fold in C1 chondrites;

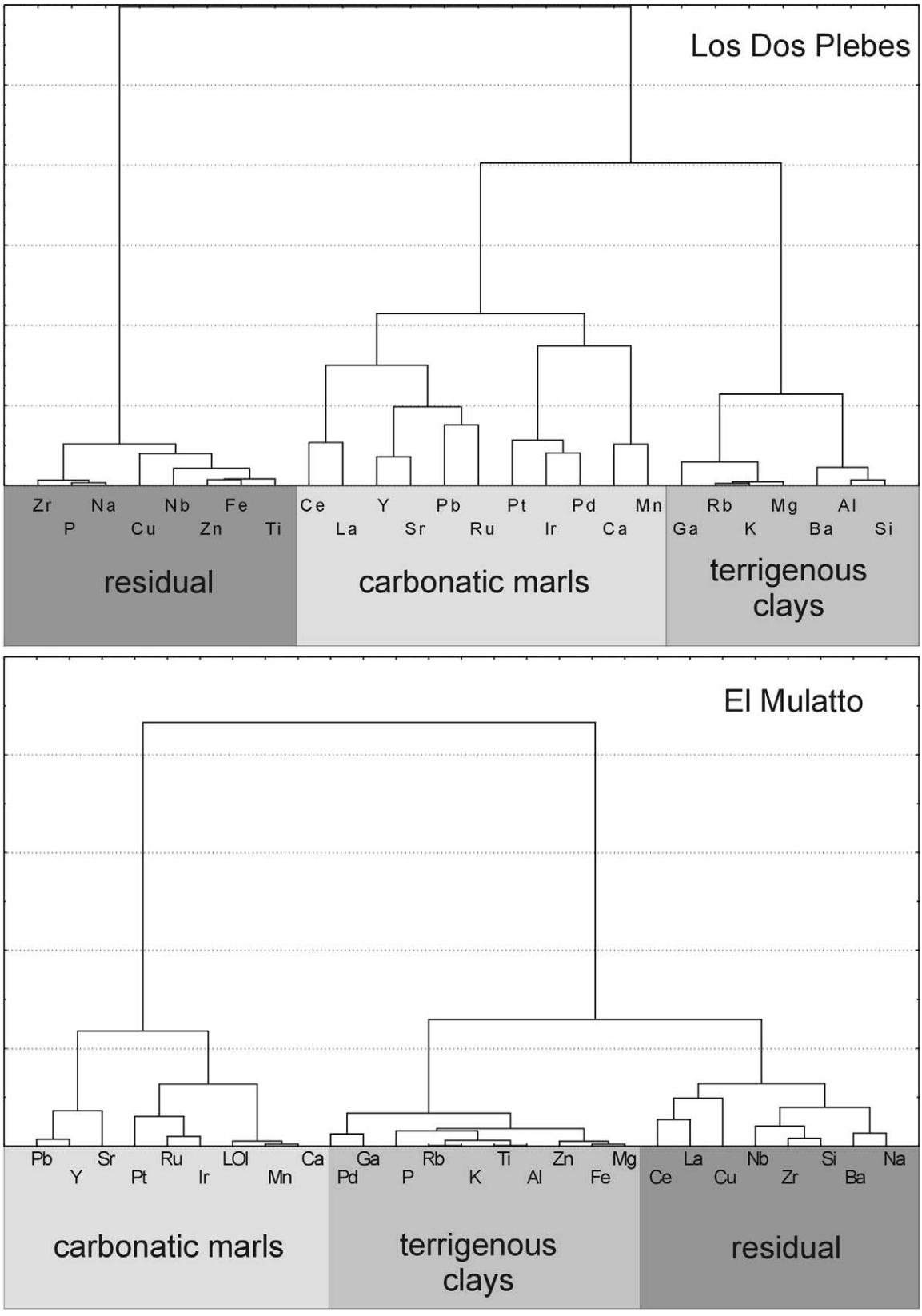

Fig. 10. R-mode hierarchical cluster analysis of major and trace elements, and PGE data for the Los Dos Plebes section and El Mulato section.

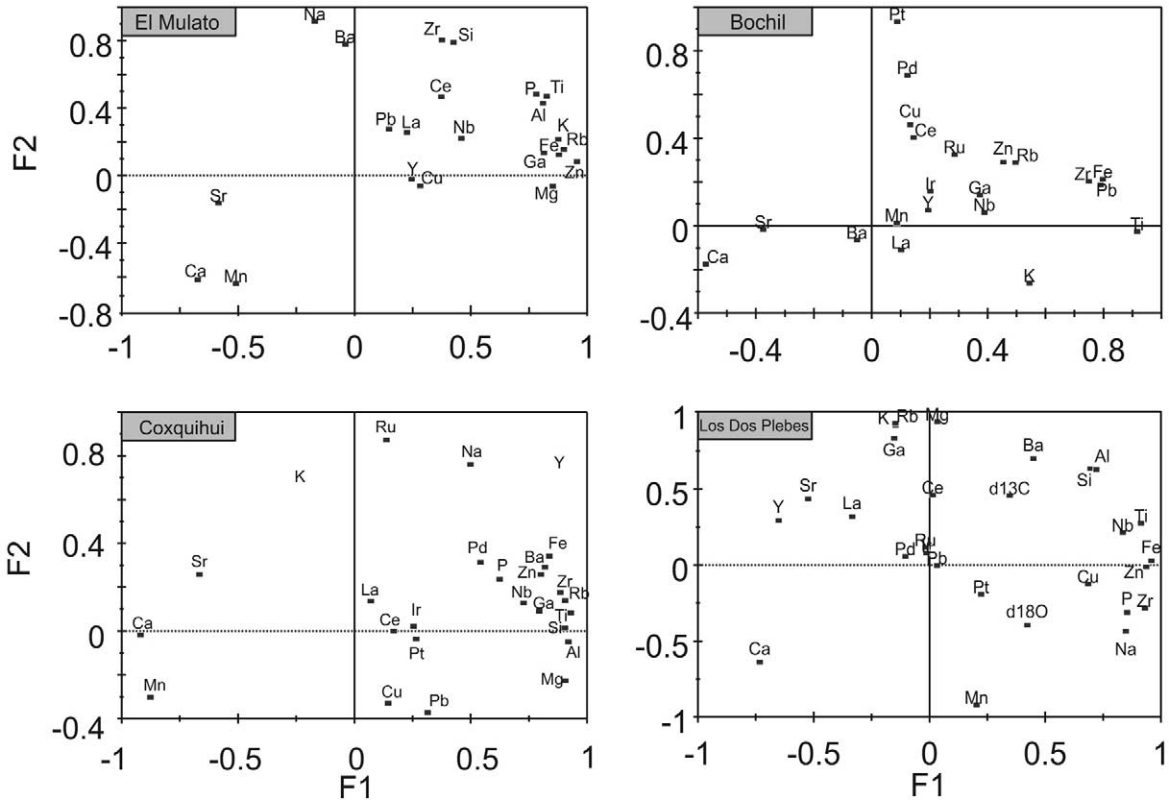

Fig. 11. Loadings of factor 1 (F1) vs. factor 2 (F2) for major and trace elements at the K/T sections at El Mulato, Bochil, Coxquihui, and Los Dos Plebes.

McDonough and Sun, 1995), high Ir contents in sedimentary rocks are used as strong indicators for meteoritic contribution. However, Ir enrichments do not originate exclusively from meteorite impacts, but also occur in Earth's mantle/mantle derived rocks, and some Ir reaches the crust via volcanic eruptions. In most cases, terrestrial anomalies and anomalies associated with meteoritic contamination (impact generated anomalies) can be differentiated by the chondrite-normalized PGE patterns (Tredoux et al., 1989; Sawlowicz, 1993; Kramar et al., 2001).

Iridium-dominated PGE anomalies are observed in K/T sections at Los Dos Plebes, El Mulato, La Lajilla, El Mimbral, Coxquihui, and Bochil. At Los Dos Plebes and La Lajilla these anomalies are extremely low (< 0.5 ng/g Ir), and in none of these sections they exceed 1.3 ng/g Ir. The chondrite-normalized PGE patterns of the Ir-dominated anomalies are roughly chondritic (Fig. 13). In some of the sections (e.g., Los Dos Plebes, La Lajilla), the very weak anomalies show slightly increased values for Pt and Pd. This can be explained by a strong dilution of a possible bolide component by material with background concentrations and crustal PGE patterns. Due to this dilution, the meteoritic PGE pattern may be overprinted by the normal terrestrial PGE pattern (Kramar et al., 2001; Stüben et al., 2002). Based on their nearly chondritic PGE patterns, the Ir-dominated PGE anomalies in the sections at Los Dos Plebes, El Mulato, La Lajilla, Coxquihui, and Bochil and also the anomaly reported for El Mimbral (Keller et al., 1994), probably originate from the K/T impact event. In all sections the Ir-dominated anomaly is bound to a clay layer which is stratigraphically separated from the spherule layer at the base of the siliciclastic deposit (unit 1), and is also separated from the rippled sandy limestone layer that frequently marks the top of unit 3 of this deposit.

The Bochil and Coxquihui sections display a second Pt, Pd dominated PGE enrichment, which is separated by 20 cm and 80 cm, respectively, from the Ir-dominated anomaly. In the K/T sections of Beloc/Haiti, it could be shown that a second anomaly of probable volcanic origin is present close to, but clearly separated from the impact-induced Ir anomaly (Kramar et al., 2001; Stüben et al., 2002). The stronger enrichment of Pd compared to Pt at Coxquihui and Bochil argues for hydrogenetic precipitation or mobilization rather than for a volcanogenic origin.

In all sections the PGE anomalies (Ir and Pt, Pd dominated) are accompanied by increasing concentrations of elements which are preferentially bound to residual phases, reflecting increased input of detrital material or reduced carbonate productivity. Mexican K/T boundary sections present a maximum of 1.3 ng/g Ir and are thus much less enriched in this element than sections in Europe and Tunisia, although these localities are more distant to the suggested K/T boundary impact crater on the Yucatán peninsula. For instance, Ir concentrations reach 48 ppb at Stevens Clint, 56 ppb at Caravaca (Tredoux et al., 1989), 8 ppb at Gubbio (Alvarez, 1987), and 23 ppb at El Kef (Rocchia and Robin, 1998). At all these locatalities the chon-

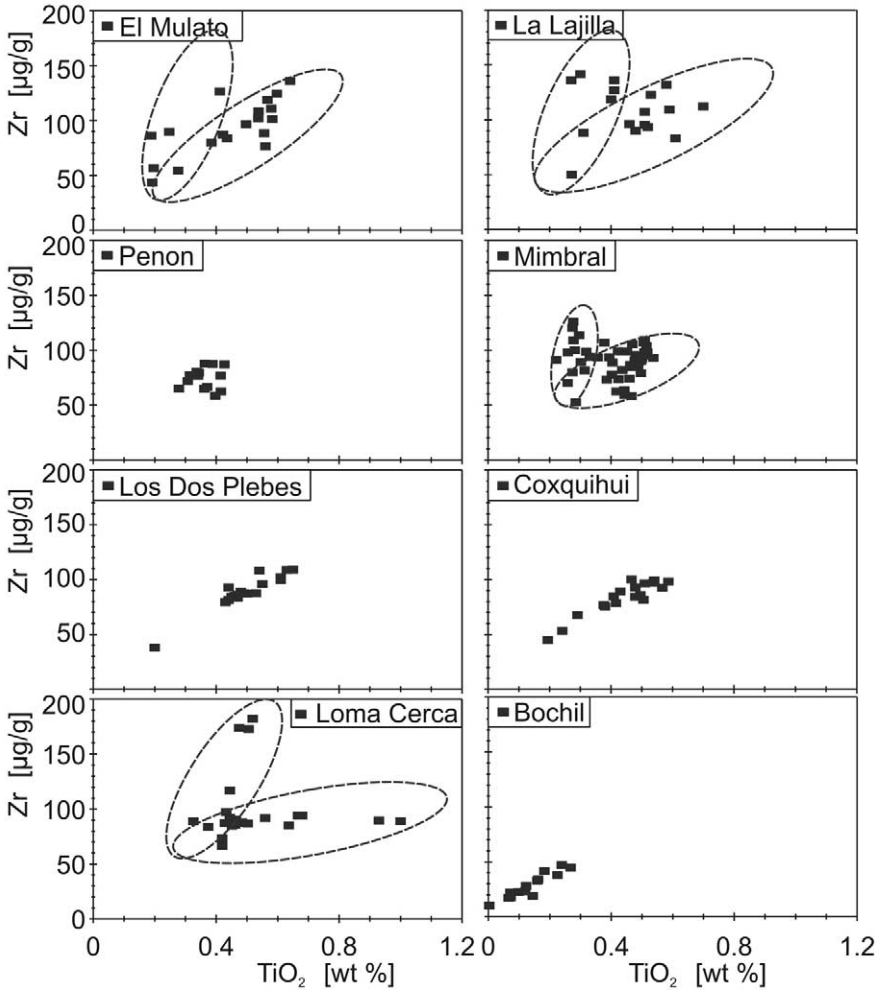

Fig. 12. Zr/Ti scatter plots as indication for changing sources of detrital sediment. Note: A simple linear correlation indicates the mixing line between a single terrigenous source and marine sediments. At Mimbral, Loma Cerrca, El Mulato, and La Lajilla the separation of the Zr/Ti ratio into two or more significantly correlating groups within one section is evident for changing sources of material for the detrital sediment component (Zr in ppm, TiO_2 in wt.%).

drite-normalized PGE patterns are nearly flat, indicating an impact origin for the PGE anomalies.

Based on the lithostratigraphic, geochemical, and mineralogical data, the Ir-dominated PGE anomaly is clearly separated from the spherule-rich deposits of unit 1 or in the Mendez marls. At La Lajilla, Los Dos Plebes, El Mulato, Bochil, and Coxquihui, the Ir-dominated anomaly shows an approximately chondritic PGE pattern (Fig. 13) and is present above and stratigraphically separated from the spherule-rich layer. At La Lajilla, El Mulato, and El Mimbral, the spherule layer is below and the Ir anomaly above the siliciclastic deposit. Several horizons of trace fossil assemblages, including *domichnia* (e.g., *Ophiomorpha, Thalassinoides*) and *fodichnia* (e.g., *Chondrites*, *Zoophycos*), indicate that deposition required a long period of time and could not have been the result of a tsunami (Keller et al., 1997; Ekdale and Stinnesbeck, 1998). Consequently, these burrows provide crucial evidence for deposition of the spherules long before the extinction of planktic foraminifera and deposition of the Ir anomaly. In several sections (Bochil, La Lajilla, El Mulato, and Coxquihui), maximum Pd concentrations occur separated from the maximum Ir and Pt concentration in different layers. Because Pd is more mobile than other PGEs (Sawlowicz, 1993), this element can be separated by local mobilization and readsorption by clay minerals (e.g., smectite or by hydrogenetic deposition). This interpretation is supported by the results of cluster and factor analysis for the Bochil, La Lajilla, El Mulato, and Coxquihui sections where Pd is clearly separated from the other PGEs (Figs. 10 and 11) and assigned to the pelitic group. Therefore, stratigraphically separated Pd enrichments are not indicative for either volcanic activity or a meteorite impact, but may result from hydrogenetic deposition or mobilization and readsorption. Moreover, volcanic activity is not necessarily accompanied by PGE enrichment.

At El Peñon and Loma Cerca, sediments above the siliciclastic deposit are eroded and no Ir anomaly has been recognized by us or other authors in the rippled sandy limestone forming the top of this deposit. The source of Ir content in these samples is mainly from the cosmogenic background of micrometeorites (Bruns et al., 1996). The occurrence of Ir together

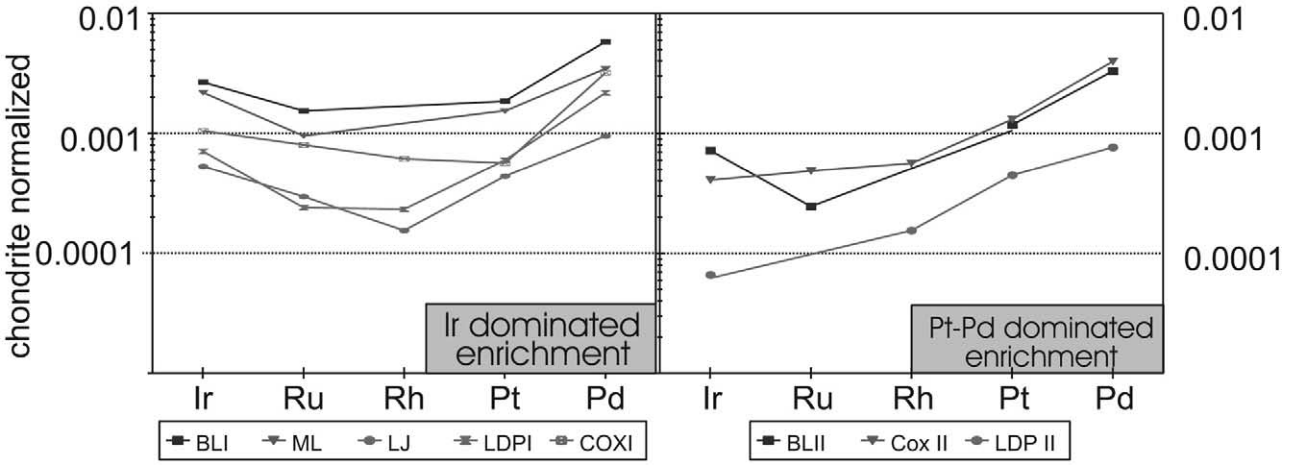

Fig. 13. Chondrite-normalized PGE patterns for the Ir-enriched layers (left) of Bochil (BLI), El Mulato (ML), La Lajilla (LJ), Los Dos Plebes (LDPI), and Coxquihui (COXI) indicating impact-induced origin, and of the PT/Pd dominated PGE-enriched layers (right) of Bochil (BLII), Los Dos Plebes (LDPII), and Coxquihui (COXII) indicating volcanogenic or hydrogenetic origin.

with detrital components (factor 2) may be due to changing dilution of the cosmogenic background component with biogenic carbonate. At Loma Cerca and El Peñon, as well as in numerous other sections in NE Mexico, multiple spherule layers can be observed (Stinnesbeck et al., 2001; Keller et al., 2002a, 2003). These regionally distributed multiple spherule layers which are interlayered in latest Maastrichtian marls of Zone *P. hantkeninoides* (CF1), are crucial to the interpretation of a pre-K/T age for the Chicxulub impact (Stinnesbeck et al., 2001; Keller et al., 2002a, 2003, 2004a,b). The lowermost layer represents the original impact fallout deposit, as indicated both biostratigraphically and mineralogically (e.g., no detritus and only rare reworked clasts), whereas layers upsection are considered reworked material derived from this layer (it contains an abundance of shallow water detritus and clasts). The regional presence of the multiple spherule layers also excludes interpretation as deposits caused by soft sediment deformation as discussed by Soria et al. (2001) and Schulte et al. (2003) for some sections of the Mesa Juan Perez outcrop area.

The timing of deposition of the (multiple) spherule layers and the impact-induced PGE anomaly is important to determine whether one or more impact events occurred. To distinguish between altered volcanoclastic sediments and altered terrigenous sediments, a discrimination diagram according to Andreozzi et al. (1997) was used (Fig. 14). Regarding the investigated K/T sections, nearly all samples plot into the field of terrigenous sediments. At El Mimbral the samples from a bentonite layer 50 cm above the K/T boundary are separated from the sedimentary field and appear in the volcanic field (Fig. 14). This represents a thin ash layer deposited well after the Chicxulub impact. The regionally observed additional PGE anomaly in the early Danian zone Pla (e.g., Coxquihui, Bochil, Beloc, Haiti; Stüben et al., 2002), which is Pt, Pd dominated with only slightly increased Ir concentration, could represent an additional tracer of volcanic activity.

At Los Dos Plebes the samples from a reddish siltstone layer 40 cm below and one sample 40 cm above the sandstone also plot into the volcanic field (Fig. 14). The samples of this siltstone layer and from a few centimeters above and below are slightly enriched in Pt and Pd, but not in Ir. The samples of the K/T boundary layer and a few centimeters above and below in all sections clearly plot in the sedimentary sector. Therefore,

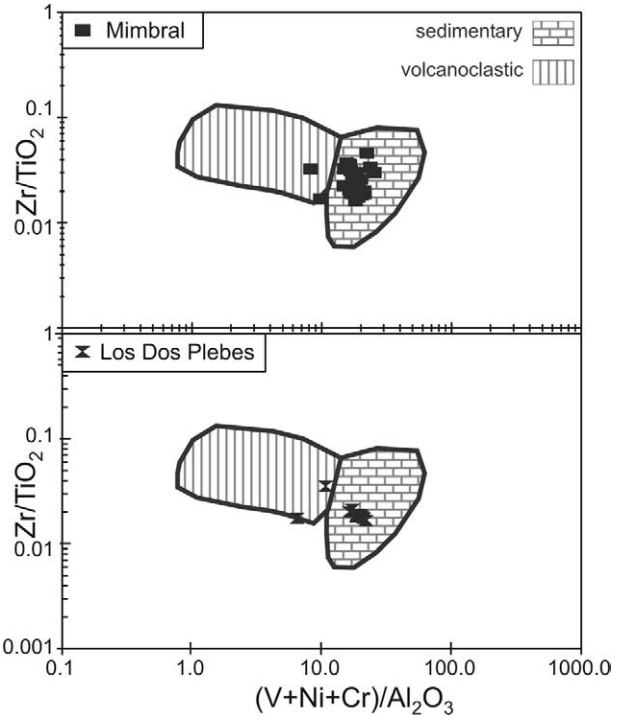

Fig. 14. Discrimination of volcanogenic and sedimentary components based on Zr/TiO_2 vs. $(V+Ni+Cr)/Al_2O_3$ within the sedimentary K/T sections at Mimbral and Los Dos Plebes (after Andreozzi et al., 1997). Within the sections, layers of only few centimeters thickness contain volcanic ashes, therefore only a few samples plot into the volcanoclastic field.

the anomalies at the K/T boundary layer are not of volcanogenic origin. The impact component in the sediments is however too small to show up as its own group in the discrimination diagram according to Andreozzi et al. (1997).

The chondrite-normalized PGE patterns (Kramar et al., 2001) for the investigated sections (Fig. 13) indicate that the Pt-Pd dominated anomalies are indicative of terrestrial origin and are clearly different from cosmogenic sources. Sediments with volcanogenic components as discriminated according to the diagram of Andreozzi et al. (1997), and the presence of Pt-Pd dominated PGE anomalies are indicative for volcanic activities before and after the K/T event. In the K/T boundary layer neither a volcanic source nor a strong meteoritic Ir anomaly can be observed, but this may be due to the generally incomplete K/T boundary interval in Mexico.

7. PALEORECONSTRUCTION OF THE SEDIMENTOLOGICAL ENVIRONMENT

Trace element and mineralogical studies can provide important information concerning the paleoenvironmental consequences of the Chicxulub impact, its relation to the K/T transition in NE Mexico and characterization of the sedimentological settings. The concentrations of major and trace elements in the analyzed sections show considerable variations reflecting varying sources, as well as different flux rates, genetic effects, and depositional environments. Calcium, Sr, Mg, and Cd are partly incorporated into biogenic carbonates. The major part of Ti, Al, Cr, K, and Fe are bound to the lattice of terrigenous debris (Murray and Leinen, 1993), whereas Ti is the most stable and immobile component unaffected by weathering. Calcium carbonate, as the main component for the primary biogenic sedimentation, as well as Zr and TiO_2 for the terrigenous sedimentation, can be used as proxies for the amount of terrigenous vs. biogenic-carbonate components. The abundance of Ba and Sr in sediments is controlled by various factors, including terrigenous flux, biogenic flux, and hydrothermal input (Murray and Leinen, 1993; Schroeder et al., 1997).

The "excess" ratio $R = El^*/El_{total}$ is used to estimate the variation of the amount of nondetrital components in the sediments across the sections. The excess ratios may give information about the fraction of an element bound to the biogenic part of the sediments. Nevertheless excess ratios can be affected by diagenesis. Strongly negative excess values ore observed in cases where the element/Ti ratio of the detritic source is lower than NASC or PAAS values. The excess ratios of Ba (R_{Ba}) in the La Lajilla section (Fig. 6) are relatively constant up to 20 cm below the Ir anomaly at the K/T boundary. Over these 20 cm, a steady decrease of R_{Ba} is observed with a minimum at a few centimeters below the PGE anomaly. A slight increase is observed ~5 cm above this interval, exactly above the K/T boundary. In P1a(1) R_{Ba} remains at a low level. Formation of diagenetic barite or barium feldspar would produce high excess ratios. The other excess ratios fluctuate in the siliciclastic deposit below the K/T boundary, indicating changes of sediment sources, terrigenous flux, and postdepositional changes. Above the K/T boundary, nearly constant excess ratios indicate monotonous sedimentation for the Danian Velasco marls (Figs. 2–9). Trace elements at Los Dos Plebes (Fig. 2) show a similar behavior below the K/T boundary but a positive excursion of R_{Ba} coincident with the PGE anomaly, which may be due to diagenetic barite formation. A slight decrease of all excess ratios during the 20 cm above the K/T boundary is followed by monotonous sedimentation in the P1a marl sequence. At El Mulato (Fig. 5) scattering excess ratios are observed up to 20 cm above the Ir anomaly, which reflects considerable changes in detrital and biogenic sedimentation. Above this interval, sedimentation returns to more monotonous conditions with low R_{Ba}. The excess ratios indicate monotonous sedimentation of the marls. Significant variations of the excess ratios are restricted to the spherule layers. The breccia interval of the Bochil section shows scattering excess ratios reflecting rapidly varying amounts of detrital material or diagenetic overprints (Fig. 9).

Correlating the excess ratios for all sections, a general reduction of the R-values at the K/T transition becomes evident when compared with late Maastrichtian marls (Fig. 15). This general trend argues against a diagenetic effect and instead indicates reduced bioproductivity with a slow recovery in the Paleocene, which confirms the microfossil evidence. This general trend is overprinted by the complex sedimentation pattern around the K/T boundary.

Titanium and Zr are exclusively bound to the detrital phase, with the Zr/Ti ratio characteristic for the source of detrital sediments. At El Mulato, La Lajilla, Mimbral, and Loma Cerca, two groups of samples with different Zr/Ti ratios are observed (Fig. 14). Principal component analysis identifies two or three individual detrital factors representing different sources for the detrital components. This may be caused by changes in continental material delivered during the uplift of the Sierra Madre or by sea level variations. In general, the European and Tunesian K/T sections like Stevns Clint (Denmark), Gubbio (Italy), Caravaca (Spain), and El Kef (Tunisia) show a different lithological composition, as well as different trace element patterns (Ganapathy, 1980; Doehne and Margolis, 1990; Tredoux et al., 1989; Alvarez, 1987; Rocchia and Robin 1998). A detrital layer like the sandstone (unit 2) of NE Mexican K/T boundary transitions has not been described from European sections.

At Los Dos Plebes, La Lajilla, and Coxquihui (Figs. 2, 6, 8), a negative excursion in $\delta^{13}C$ at the K/T boundary is accompanied by reduced carbonate sedimentation and indicates reduced surface productivity followed by a slow recovery in the lower Paleocene. This confirms a pattern documented globally and also evident in the microfossil record. It is consistent with stable isotopic changes generally observed in Tethyan sections (e.g., Keller and Lindinger, l989; Zachos et al., l994; Stüben et al., 2002). The $\delta^{18}O$ is partly contradictory at Coxquihui and La Lajilla (Figs. 6 and 8), where a continuous increase during late Maastrichtian was followed by a rapid decrease at or near the K/T transition. The Los Dos Plebes section displays extremely negative $\delta^{18}O$ values and trends as compared with La Lajilla and Coxquihui (Figs. 2, 6, and 8), probably due to diagenetic alteration. An increase in temperature, caused by sediment burial and possibly different isotopic composition of pore fluids are the most important factors altering the primary isotopic signal of biogenic calcite (Killingley, 1983; Jenkyns

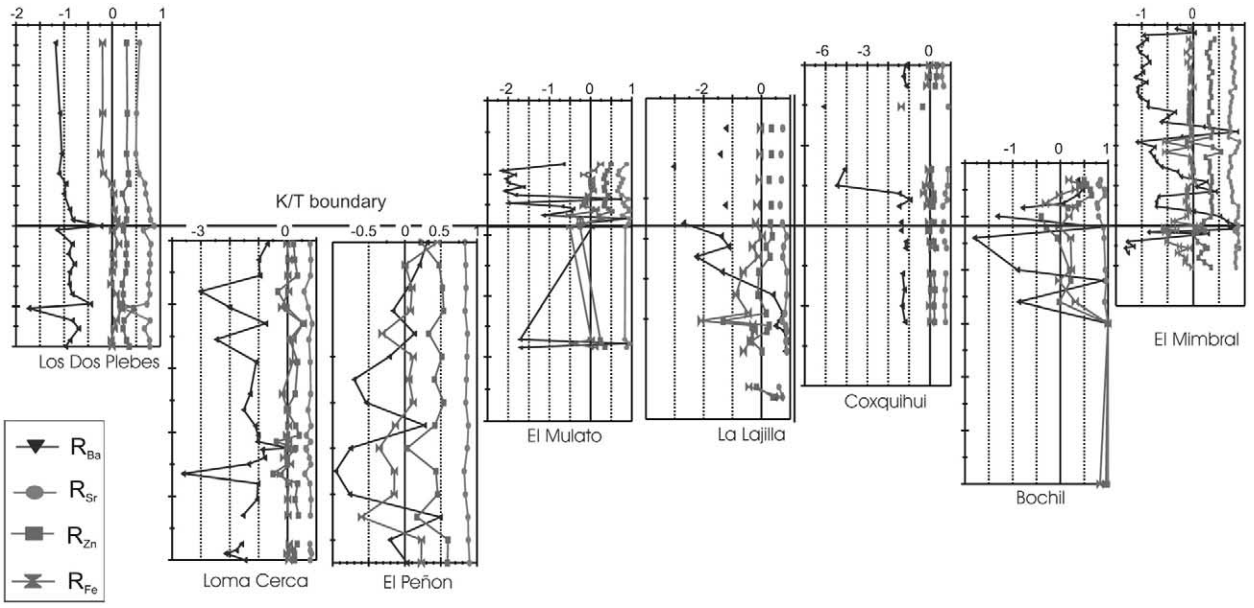

Fig. 15. Correlation of excess ratios R for the K/T sections Los Dos Plebes, Loma Cerca, El Peñon, El Mulato, La Lajilla, Mimbral, Coxquihui, and Bochil. The sections are arranged relative to the K/T boundary. At the Loma Cerca and El Peñon sections the K/T boundary is eroded, but in both multiple spherule layers are exposed in the Maastrichtian. The thick horizontal line connecting the sections marks the K/T boundary. The tick marks at the left side of each section are the depth scales from Figures 2 to 9.

et al., 1994; Schrag et al., 1995; Mitchell et al., 1997). Generally, both these factors tend to lower the initial oxygen isotopic values. Consequently, if a part of the carbonate was affected by recrystallization, the excursion towards more negative $\delta^{18}O$ values may represent diagenetically altered isotopic values, whereas higher values should be regarded as minimum values. The extremely negative $\delta^{18}O$ values within the Los Dos Plebes section suggest a strong diagenetic overprint that masks the primary isotopic signal. At Coxquihui and La Lajilla the oxygen isotope trend suggests cooling during the latest Maastrichtian, except for two anomalous values of −6‰, −7‰, followed by a rapid temperature change at or near the K/T boundary and a slight recovery in the lower Danian.

8. CONCLUSIONS

Trace elements, PGE, and isotope data from eight different K/T sections, extending north-south over 1500 km, reveal a complex sedimentation history and have implications for the relationship between the K/T boundary and the Chicxulub impact. All K/T sections investigated show one to two PGE anomalies with different chondrite-normalized PGE patterns that reflect cosmogenic and volcanogenic origins. The Ir-dominated PGE anomaly occurs always at or near the K/T boundary and marks an impact event. This impact event occurred well after the reworked spherule-rich deposit of unit 1 at the base of the siliciclastic deposits, or the position that marks the original deposition of the Chicxulub impact spherule ejecta within the underlying Mendez marl formation at the base of zone CF1. Trace element geochemistry also supports a significant amount of time passed between deposition of the spherule layers and the Ir anomaly at the K/T boundary. This supports the biostratigraphic and magnetostratigraphic finding (Keller et al., 2004a,b) that the Chicxulub impact predates the K/T boundary by ~300,000 yr.

At Mimbral, Bochil, Coxquihui, and Los Dos Plebes, Pt and Pd dominated PGE anomalies are present before and after the K/T boundary. However, different PGE-normalized patterns as well as different trace element patterns within a bentonite layer give evidence for volcanic activity. This is underlined by the discrimination diagram of Andreozzi et al. (1997), which is based on an element group of volcanogenic origin and their weathering behavior. Isolated Pd enrichments in various layers are always correlated with elements that are commonly bound to clay minerals. Consequently these Pd enrichments have to be interpreted as remobilization and coprecipitation on clay minerals.

Major and trace element geochemistry indicates a complex sedimentation history. In the El Mimbral, La Lajilla, Bochil, and El Peñon sections, a Ba peak decoupled from other trace elements is observed and could be a helpful indicator for changes in the deposition environment. However, the origin and interpretation of these Ba peaks is not well constrained. The different characteristic Zr/Ti ratios indicate changing sources of terrestrial input or changing paleoenvironmental conditions. Major and trace element trends within the sections, as well as the calculation of the excess ratios, indicate variable influx of biogenic to detrital sedimentation due to changing distance to shore lines, variable water depths, and sources of detrital sediments. Carbon and oxygen isotope studies as well as trace element data

indicate a gradually changing climate near the end of the Cretaceous and an abrupt change at the K/T boundary followed by a slight recovery during the lowermost Paleocene.

Acknowledgments—This study was supported by the Deutsche Forschungsgemeinschaft (grants Sti 128/2 and 128/7 and Stu 169/10-1-3), the National Science Foundation (grant OCE-9021338), and the Petroleum Research Fund (ACS-PRF grant 2670-AC8). Falk Lindenmaier provided PGE data of Los Dos Plebes and La Lajilla. We thank Dr. José Guadalupe López-Oliva, Linares, for valuable suggestions, discussions, and help during our field work in NE Mexico. We also thank the staff of our laboratory—Gesine Preuss, Claudia Möβner, Peter Schaupp, Manfred Gerken, and Stefan Höhne. Without their efforts this investigation would not have been possible. We thank Uwe Reimold and Henning Dypvik, and two anonymous reviewers, for their helpful suggestions and comments.

Associate editor: W. U. Reimold

REFERENCES

Adatte T., Stinnesbeck W., and Keller G. (1996) Lithostratigraphic and mineralogic correlations of near K/T boundary clastic sediments in NE Mexico: Implications for origin and nature of deposition. In *The Cretaceous–Tertiary Boundary Event and Other Catastrophes in Earth History* (eds. G. Ryder, D. Fastovsky, and S. Gartner) *Geol. Soc. Am. Spec. Paper* **307**, 211–226.

Alegret L., Arenillas I., Arz J. A., Liesa C., Mélendez A., Molina E., Soria A. R., and Thomas E. (2002) The Cretaceous/Tertiary boundary: Sedimentology and micropaleontology at the El Mulato section, NE Mexico. *Terra Nova* **14,** 330–336.

Alvarez L. W. (1987) Mass extinction caused by large bolide impacts. *Physics Today* **40,** 24–33.

Alvarez W., Smit J., Lowrie W., Asaro F., Margolis S. V., Claeys P., Kastner M., and Hildebrand A. R. (1992) Proximal impact deposits at the Cretaceous–Tertiary boundary in the Gulf of Mexico: A restudy of DSDP Leg 77 Sites 536 and 540. *Geology* **22,** 697–700.

Andreozzi M., Dinelli E., and Tateo F. (1997) Geochemical and mineralogical criteria for the identification of ash layers in the stratigraphic framework of a fordeep: The Early Miocene Mt. Cervarola Sandstones, northern Italy. *Chem. Geol.* **137,** 23–39.

Arz J. A., Arenillas I., Soria A. R., Alegret L., Grajales-Nishimura J. M., Liesa C. L., Melendez A., Molina E., and Rosales M. C. (2001) Micropaleontology and sedimentology across the Cretaceous/Tertiary boundary at La Ceiba (Mexico): Impact-generated sediment gravity flows. In *Geology of Northwestern Mexico and Adjacent Areas* (eds. C. M. Gonzalez-Leon and A. M Barajas). *J. South Amer. Earth Sci.* **14** (*5*), 505–519.

Arz J. A., Alegret L., and Arenillas I. (2004) Foraminiferal biostratigraphy and paleoenvironmental reconstruction at Yaxcopoil-1 drill hole, Chicxulub crater, Yucatán Peninsula. *Meteor. Planet. Sci.* **39,** l099–1111.

Bach W. and Irber W. (1998) Rare earth element mobility in the oceanic lower sheeted dyke complex: Evidence from geochemical data and leaching experiments. *Chem. Geol.* **151,** 309–326.

Berner Z., Stüben D., Leosson M. A., and Klinge H. (2001) S- and O-isotopic character of dissolved sulfate in the cover rock aquifers of a Zechstein salt dome. *Appl. Geochem.* **17,** 1515–1528.

Bohor B. F. (1996) A sediment gravity flow hypothesis for siliciclastic units at the K/T boundary, northeastern Mexico. In *The Cretaceous–Tertiary Boundary Event and Other Catastrophes in Earth History* (eds. G. Ryder, D. Fastovsky, and S. Gartner). *Geol. Soc. Am. Spec. Paper* **307,** 183–195.

Bohor B. F. and Betterton W. J. (1993) Arroyo el El Mimbral, Mexico, K/T unit: Origin as debris flow/turbidite, not a tsunami deposit. *Lunar Planet. Sci. Conf.* **24,** 143–144.

Bruns P., Dullo W.-C., Hay W. W., Wold C. N., and Pernicka E. (1996) Iridium concentration as an estimator of instantaneous sediment accumulation rates. *J. Sed. Res.* **66,** 608–612.

Claeys P., Kiessling W., and Alvarez W. (2002) Distribution of Chicxulub ejecta at the Cretaceous–Tertiary boundary. In *Catastrophic Events and Mass Extinctions: Impacts and Beyond* (eds. C. Koeberl and K. G. McLeod). *Geol. Soc. Am. Spec. Paper* **356**, 55–68.

Cowie J. W., Ziegler W., and Remane J. (1989) Stratigraphic Commission accelerates progress, 1984–1989. *Episodes* **12** (*2*), 79–83.

Doehne E. and Margolis S. V. (1990) Trace element geochemistry and mineralogy of the Cretaceous/Tertiary boundary: Identification of extraterrestrial components. *Geol Soc. Am. Spec. Pap.* **247,** 367–382.

Ekdale A. A. and Stinnesbeck W. (1998) Trace fossils in Cretaceous–Tertiary (KT) boundary beds in northeastern Mexico: Implications for sedimentation during the KT boundary event. *Palaios* **13,** 593–602.

Galloway W. E. and Williams T. A. (1991) Sediment accumulation rates in time and space: Paleogene genetic stratigraphic sequences of the northwestern Gulf of Mexico basin. *Geology* **19** (*10*), 986–989.

Ganapathy R. (1980) A major meteorite impact on the Earth 65 million years ago: Evidence from the Cretaceous–Tertiary boundary clay. *Science* **209,** 921–923.

Govindaraju K. (1995) Update (1984–1995) on two GIT-IWG geochemical reference samples; albite from Italy, AL-I and iron formation sample from Greenland, IF-G. *Geostandards Newsletter* **19** (*1*), 55–96.

Grajales-Nishimura J. M., Cedillo Pardo E., Rosales-Dominguez C., Moran-Zenteno D. J., Alvarez W., Claeys P., Ruiz-Morales J., Garcia-Hernandez J., Padilla-Avila P., and Sanchez-Rios A. (2000) Chicxulub impact; the origin of reservoir and seal facies in the southeastern Mexico oil fields. *Geology* **28** (*12*), 1152.

Gromet L. P., Dymek R. F., Haskin L. A., and Korotev R. L. (1984) The "North American shale composite": Its compilation, major and trace element characteristics. *Geochim. Cosmochim. Acta* **48,** 2469–2482.

Hannigan R. and Basu A. R. (1998) Late diagenetic trace element remobilization in organic-rich black shales of the Taconic Foreland Basin of Québec, Ontario and New York. In *Shales and Mudstones II, Petrography, Petrophysics, Geochemistry and Economic Geology* (eds. J. Schieber, W. Zimmerle and P. S. Sethi). Schweizerbart'sche Verlagsbuchhandlung, Stuttgart, pp. 209–234.

Harting M. (2004) *Zum Kreide/Tertiär-Übergang in NE-Mexiko: Geochemische Charakterisierung der Chicxulub-Impaktejekta.* Karlsruhe University Press, Karlsruhe.

Jenkins R., Gould R. W., and Gedcke D. (1981) *Quantitative X-Ray Spectrometry.* Marcel Dekker, New York.

Jenkyns H. C., Gale A. S., and Corfield R. M. (1994) Carbon- and oxygen-isotope stratigraphy of the English Chalk and Italian Scaglia and its paleoclimatic significance. *Geol. Mag.* **131,** 1–34.

Keller G. and Lindinger M. (1989) Stable isotope, TOC and $CaCO_3$ records across the Cretaceous/Tertiary boundary at El Kef, Tunisia. *Palaeogeogr. Palaeoclimatol. Palaeoecol.* **73,** 243–265.

Keller G., MacLeod N., Lyons J. B., and Officer C. B. (1993) Is there evidence for Cretaceous–Tertiary boundary-age deep-water deposits in the Caribbean and Gulf of Mexico? *Geology* **21** (*9*), 776–780.

Keller G., Stinnesbeck W., Adatte T., McLeod N., and Lowe D. R. (1994) Field guide to Cretaceous–Tertiary boundary section regarding the KT event and other catastrophes in earth history. *Lunar Planet. Inst. Cont.* **827,** 1–110.

Keller G., Li L., and MacLeod N. (1995) The Cretaceous/Tertiary boundary stratotype section at El Kef, Tunisia: How catastrophic was the mass extinction? *Palaeogeogr. Palaeoclimatol. Palaeoecol.* **119,** 222–254.

Keller G., López-Oliva J. G., Stinnesbeck W., and Adatte T. (1997) Age, stratigraphy and deposition of near-K/T siliciclastic deposits in Mexico: Relation to bolide impact? *Geol. Soc. America Bull.* **109,** 410–428.

Keller G., Adatte T., Stinnesbeck W., Luciani V., Karoui N., and Zaghbib-Turki D. (2002a) Paleoecology of the Cretaceous–Tertiary mass extinction in planktic foraminifera. *Paleogeogr. Paleoclimatol. Paleoecol.* **178,** 257–298.

Keller G., Adatte T., Stinnesbeck W., Affolter M., Schilli L., and López-Oliva J. G. (2002b) Multiple layers in the late Maastrichtian of northeastern Mexico. *Geol. Soc. Am. Spec. Paper* **356**.

Keller G., Stinnesbeck W., and Adatte T. (2002c) Slumping and a sandbar deposit at the Cretaceous–Tertiary boundary in the El Tecolote section (northeastern Mexico): An impact induced sediment gravity flow—Comment. *Geology* **30,** 382–383.

Keller G., Stinnesbeck W., Adatte T., Holland B., Stüben D., Harting M., Leon de C., and Cruz de la J. (2003) Spherule deposits in Cretaceous–Tertiary boundary sediments in Belize and Guatemala. *J. Geol. Soc. London* **160,** 783–795.

Keller G., Adatte T., Stinnesbeck W., Rebolledo-Vieyra M., Urrutia-Fucugauchi J., Kramar U., and Stüben D. (2004a) Chicxulub impact predates the K-T boundary mass extinction. *PNAS* **101** (*11*), 3721–3992.

Keller G., Adatte T., Stinnesbeck W., Kramar U., and Stüben D. (2004b) More evidence that the Chicxulub impact predates the K-T boundary mass extinction. *Meteor. Planet. Sci.* **39,** 1127–1144.

Killingley J. S. (1983) Effects of diagenetic recrystallization on $^{18}O/^{16}O$ values of deep-sea sediments. *Nature* **301,** 594–597.

Kramar U. (1997) Advances in energy-dispersive X-ray fluorescence. *J. Geochem. Explor.* **58,** 73–80.

Kramar U., Stüben D., Berner Z., Stinnesbeck W., Philipp H., and Keller G. (2001) Are Ir anomalies sufficient and unique indicators for cosmic events? *Planet. Space Sci.* **49,** 831–837.

Lachance G. R. and Claisse F. (1995) *Quantitative X-ray Fluorescence Analysis*. Wiley, New York.

Lindenmaier F., Stüben D., Kramar U., Stinnesbeck W., Keller G., and López-Oliva J. G. (1999) Chemostratigraphy of the K/T-boundary at La Sierrita and La Lajilla, NE Mexico. Geological Society of America, 1999 annual meeting. Abstracts with Programs. Geological Society of America. Boulder, CO. *Geological Society of America*, **123**.

López-Oliva J. G. and Keller G. (1996) Age and stratigraphy of near-K/T boundary clastic deposits in northeastern Mexico. In *The Cretaceous–Tertiary Event and Other Catastrophes in Earth History* (eds. G. Ryder, D. Fastovsky, and S. Gartner) *Spec. Pap. Geol. Soc. Amer.* **307,** pp. 227–242.

McDonough W. F. and Sun S. S. (1995) The composition of the Earth. *Chem. Geol.* **120,** 223–253.

McManus J., Berelson W. M., Hammond D. E., and Klinkhammer G. P. (1999) Barium cycling in the North Pacific: Implications for the utility of Ba as a paleoproductivity and paleoalkalinity proxy. *Paleoceanogr.* **14,** 53–61.

Mitchell S. F., Ball J. D., Crowley S. F., Marshall J. D., Paul C. R. C., Veltkamp C. J., and Samir A. (1997) Isotope data from cretaceous chalks and foraminifera: Environmental or diagenetic signals? *Geology* **25,** 691–694.

Montanari A., Claeys P., Asaro F., Bermudez J., and Smit J. (1994) Preliminary stratigraphy and iridium and other geochemical anomalies across the K/T boundary in the Bochil section (Chiapas, southeastern Mexico). New developments regarding the K/T event and other catastrophes in Earth history. *Lunar Planet. Inst. Cont.* **825,** 8419.

Murray R. W. and Leinen M. (1993) Chemical transport to the seafloor of the equatorial Pacific Ocean across a latitudinal transect at 135°W: Tracking sedimentary major, trace and rare earth element fluxes at the Equator and the Intertropical Convergence Zone. *Geochim. Cosmochim. Acta* **57,** 4141–4163.

Murray R. W. and Leinen M. (1996) Scavenged excess aluminum and its relationship to bulk titanium in biogenic sediment from central equatorial Pacific Ocean. *Geochim. Cosmochim. Acta* **60,** 3869–3878.

Puchelt H., Malpas T., Falloon T., Pedersen R., Eckhardt J. D., and Allan J. (1996) Ultramafic reference material from Leg 147–895D10-W. In *Proc. ODP, Sci. Results* (eds. K. Gillis, C. Mével, J. Allan, and P. Meyer) **147,** 493–496.

Remane J., Keller G., Hardenbol J., and Ben Haj Ali M. (1999) Report on the international workshop on Cretaceous-Peleogene transitions. *Episodes* **22** (*19*), 47–48.

Richter F. M. and Liang Y. (1993) The rate and consequences of Sr diagenesis in deep-sea carbonates. *Earth Planet. Sci. Lett.* **177,** 553–565.

Rocchia R. and Robin E. (1998) L'iridium à la limite Crétacé-Tertiare du site d'El Kef, Tunisie. *Bull. Soc. Géol. France* **169** (*4*), 515–526.

Rock N. M. S. (1988) *Numerical Geology.* Springer, Berlin.

Sawlowicz Z. (1993) Iridium and other platinum-group elements as geochemical markers in sedimentary environments. *Palaeogeogr. Palaeoclimatol. Palaeoecol.* **104,** 253–270.

Schrag D. P., DePaolo D. J., and Richter F. M. (1995) Reconstructing past sea surface temperatures: Correcting for diagenesis of bulk marine carbonate. *Geochim. Cosmochim. Acta* **59,** 2265–2278.

Schroeder J. O., Murray R. W., Leinen M., Pflaum R. C., and Janacek T. R. (1997) Barium in equatorial Pacific carbonate sediment: Terrigenous, oxide and biogenic associations. *Palaeogeogr. Palaeoclimatol. Palaeoecol.* **12** (*1*), 125–146.

Schulte P., Stinnesbeck W., Stüben D., Kramar U., Berner Z., Keller G., and Adatte T. (2003) Fe-rich and K-rich mafic spherules from slumped and channelized Chicxulub ejecta deposits in the northern La Sierrita area, NE Mexico. *Int. J. Earth Sci.* **92** (*1*), 114–142.

Smit J., Montanari A., Swinburne N. H. M., Alvarez W., Hildebrand A., Margolis S. V., Claeys P., Lowrie W., and Asaro F. (1992) Tektite-bearing deep-water clastic unit at the Cretaceous–Tertiary boundary in northeastern Mexico. *Geology* **20,** 99–103.

Smit J., Montanari A., and Alvarez W. (1994) Tsunami-generated beds at the K/T boundary in northeastern Mexico. In *Field Guide to Cretaceous–Tertiary Boundary Sections in Northeastern Mexico* (eds. G. Keller, W. Stinnesbeck, T. Adatte, J. G. López-Oliva, and N. MacLoed). *Lunar Planet. Inst. Cont.* **827,** 1–110.

Smit J., Alvarez W., Montanari A., Clayes P., and Grajales-Nishimura J. M. (1996) Coarse-grained clastic sandstone complex at the K/T boundary around the Gulf of Mexico: Deposition by tsunami waves induced by the Chicxulub impact? In *The Cretaceous–Tertiary Boundary Event and Other Catastrophes in Earth History* (eds. G. Ryder, D. Fastovsk, and S. Gartner). *Geol. Soc. Am. Spec. Paper* **307,** 151–182.

Smit J. (1999) The global stratigraphy of the Cretaceous–Tertiary boundary impact ejecta. *Ann. Rev. Earth Planet. Sci.* **27,** 75–113.

Smit J., Van der Gaast S., and Lustenhouwer W. (2004) Is the transition impact to post-impact rock complete? Some remarks based on XRF scanning, electron microprobe and thin section analyses of the Yaxcopoil-1 core in the Chicxulub crater. *Meteor. Planet. Sci.* **39,** 1113–1126.

Sohl N. F., Martinez R. E., Salmeron-Urena P., and Soto-Jaramillo F. (1991) *Upper Cretaceous–The Gulf of Mexico Basin.* Geol. Soc. Am. Boulder, pp. 205–244.

Soria A. R., Liesa C. L., Mata M. P., Arz J. A., Alegret L., Arenillas I., and Meléndez A. (2001) Slumping and a sandbar deposit at the Cretaceous–tertiary boundary in the El Tecolote section (northeastern Mexico): An impact-induced sediment gravity flow. *Geology* **29,** 231–234.

Stinnesbeck W., Barbarin J. M., Keller G., López-Oliva J. G., Pivnik D. A., Lyons J. B., Officer C. B., Adatte T., Graup G., Rocchia R., and Robin E. (1993) Deposition of channel deposits near the Cretaceous–Tertiary boundary in northeastern Mexico: Catastrophic or "normal" sedimentary deposits. *Geology* **21,** 797–800.

Stinnesbeck W. and Keller G. (1996) Environmental changes across the Cretaceous–Tertiary Boundary in northeastern Brazil. In *The Cretaceous–Tertiary Boundary Mass Extinction. Biotic and Environmental Events* (eds. N. MacLeod and G. Keller). Norton Press, New York, pp. 51–469.

Stinnesbeck W., Keller G., Adatte T., López-Oliva J. G., and MacLeod N. (1996) Cretaceous–Tertiary boundary clastic deposits in NE Mexico: Impact tsunami or sea-level lowstand? In *The Cretaceous–Tertiary Mass Extinction: Biotic and Environmental Effects* (eds. N. MacLeod and G. Keller). Norton Press, New York, pp. 471–518.

Stinnesbeck W., Schulte P. Lindenmaier F., Adatte T., Affolter M., Schilli L., Stüben D., Berner Z., Kramar U., and López-Oliva J. G. (2001) Late Maastrichtian age of spherule deposits in northeastern Mexico: Implication for Chicxulub scenario. *Can. J. Earth Sci.* **38,** 229–238.

Stinnesbeck W., Keller G., Schulte P., Stüben D., Berner Z., Kramar U., and Guadalupe López-Oliva J. (2002) Cretaceous–Tertiary (K/T) boundary transition at Coxquihui, state of Veracruz, Mexico: Evidence for an early Danian impact event? *South Amer. Earth Sci.* **15,** 497–509.

Stüben D., Kramar U., Berner Z., Eckhardt J.-D., Stinnesbeck W., Keller G., Adatte T., and Heide K. (2002) Geochemical evidence for multiple events across the KT-boundary at Beloc, Haiti. *Geological Society of America Special Paper* **356,** 163–188.

Stüben D., Kramar U., Berner Z., Meudt M., Keller G., Abramovich S., Adatte T., Hambach U., and Stinnesbeck W. (2003) Late Maastrichtian paleoclimatic and paleoceanographic changes inferred from Sr/Ca ratio and stable isotopes. *Palaeogeogr. Palaeoclimatol. Palaeoecol.* **199,** 107–127.

Taylor H. (2000) *Inductively Coupled Plasma–Mass Spectrometry.* Elsevier, Amsterdam.

Taylor S. R. and McLennan S. M. (1985) *The Continental Crust: Its Composition and Evolution.* Oxford, Blackwell.

Tredoux M., De Wit M. J., Hart R., Lindsay N. M., Verhagen B., and Sellschop J. P. F. (1989) Chemostratigraphy across the Cretaceous–Tertiary Boundary and a critical assessment of the Iridium Anomaly. *J. Geol.* **97,** 585–605.

Zachos J., Stott L., and Lohmann K. (1994) Evolution of early Cenozoic marine temperatures. *Paleoceanogr.* **9** (*2*), 353–387.